let で作成した.

ユーザーは自身のコンピュータにバージョン6以上の Internet Explorer (Microsoft Co., U.S.A.) と化学構造を表示するためのプラグイン MDL Chime (MDL Information Systems, Inc., U.S.A.) をあらかじめインストールしておくことにより，化合物とタンパク質の立体構造を表示することができる．この立体構造はマウスで自由に回転，拡大縮小等を行うことができる.

### Web サイト検索方法

本研究で開発した *Ki*Bank は，2003 年 10 月 1 日から下記の URL で公開している.

http://kibank.iis.u-tokyo.ac.jp/

2004 年 4 月現在，*Ki*Bank は膜受容体と核内受容体から選び出した 37 種類（サブタイプとして 147 種類）の標的タンパク質について 6000 以上の結合親和性情報を保有し，1700 個以上の化合物の三次元座標データと 25 個のタンパク質の三次元座標データを蓄積している.

以下に *Ki*Bank の簡単な検索方法を示した.

*Ki*Bank のホームページ（Fig. 2(A)）から "Search *Ki*Bank" を選択して検索ページに入ると，検索のための条件を設定する画面が表示される (Fig. 2(B))．検索ページ上部には結合親和性情報やタンパク質の基礎データを検索するためのコンポーネントがあり，下部には化合物を検索するためのコンポーネントが配置されている.

検索ページ上部で受容体名をリストから選択し，検索する情報として "Binding Affinity Data" を選択すると，選択した受容体に結合する化合物名とそれぞれの $K_i$ 値の一覧表が表示される (Fig. 2(C))．ここに表示される内容は，一覧表の左から化合物名，$K_i$ 値，動物名，週齢・大きさ，性別，使用組織，実験方法，トレーサー名，緩衝液，水素イオン濃度 (pH)，参照文献の PubMed[2] ID (PMID) となっている．化合物は $K_i$ 値について昇順，すなわち結合親和性が高い順に表示されている.

この検索結果画面に表示されている化合物名の下に "3D File" ボタンが表示されている場合は，化

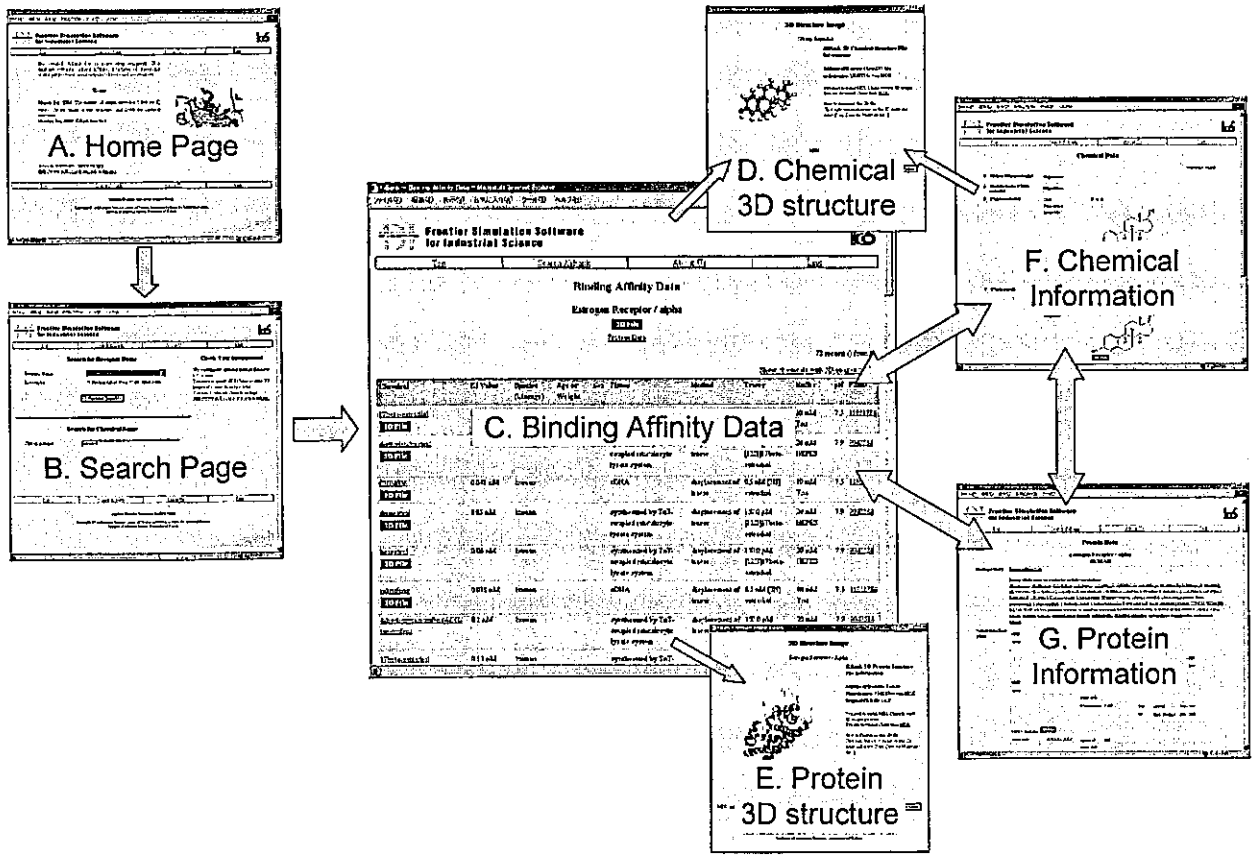


Fig. 2. A Schematic Diagram of *Ki*Bank Search Flow

合物の立体構造を表示することができる（Fig. 2 (D)）．また，受容体名の下に“3D File”ボタンがある場合は，タンパク質の立体構造イメージを表示することができる（Fig. 2(E)）．

検索結果中の化合物名をクリックすると，この化合物に関するより詳細な情報が表示され，ここには化合物の分子量，分子式，その化合物と結合する受容体の一覧などが含まれている（Fig. 2(F)）．受容体名の下にある“Protein Data”をクリックすると，PDB,[7] Protein Information Resource,[13] Swiss-Prot,[14] GenBank,[15] Genome Database,[16] dbSNP,[17] Online Mendelian Inheritance in Man (OMIM),[18] TRANSFAC[19] などへのリンク情報など，標的タンパク質に関する情報が表示される．また，このページからアミノ酸又は塩基配列の類似性比較のための Basic Local Alignment Search Tool (BLAST)[20] を実行することもできる（Fig. 2(G)）．さらに，PMID をクリックすると PubMed[2] に接続してデータソースとして使用した文献の要旨を閲覧することができる．

なお，図には示していないが，検索ページから直接化合物やタンパク質の詳細情報を検索することもできる．すべての情報はお互いにリンクされているので，どこから検索を始めても目的とする結果を得ることができる．

## 結果及び考察

現在の新薬開発は，ゲノミクス研究に基づく標的タンパクの探索（target hunting），指向する標的の評価（target validation），多数の化合物の合成（combinatorial chemistry）と能率的なスクリーニング（high-throughput screening）によるリード化合物の探索と言う過程を踏むことが多い．

この中で特に時間と労力を必要とする作業は，化合物の合成とスクリーニングである．この段階のスピードアップを図る試みとして，コンピュータを用いた分子計算により化合物の生理活性を推測する“virtual (*in silico*) screening”の方法が研究されている．Virtual screening が効果的に機能するためには，計算結果を評価するための標的タンパク質と化合物の生理活性に関するデータが必須である．そこでわれわれは，標的タンパク質と化合物の三次元座標データ，及び標的タンパク質に対する結合親和性データを一括して提供するデータベース（*Ki*Bank）の構築を行った．

標的タンパク質としてはさまざまなものが知られているが，多くの既存医薬品の標的となっている受容体タンパク質に関するデータを収集することから着手した．

受容体と結合して効果を発現する化合物の薬理学的評価は，化合物と受容体の結合親和性や，化合物が受容体に結合したのちに起こるさまざまな現象を指標として行われる．このため，公表された論文中の実験結果の記載も多様である．化合物とタンパク質の相互作用解析プログラムとして種々のドッキングソフトウェアが開発されているが，*in silico* スクリーニングではコンピュータ上で仮想的に化合物をタンパク質に結合させ，その複合体の安定化エネルギーを算出する．これは化合物と受容体の単純な結合親和性の実験と対応していると考えられる．そこで *Ki*Bank では，受容体結合実験に基づく結合親和性のみを生理活性の指標として採用することとした．

受容体に対する化合物の結合親和性の指標としては，解離定数（$K_D$），結合阻害定数（$K_i$），50%結合阻害濃度（$IC_{50}$），相対的結合親和性（relative binding affinity, RBA）などが使用されている．$K_D$ 値は放射性同位元素で標識した被験化合物と標的タンパク質の飽和曲線を作成して算出するのに対し，$K_i$ 値，$IC_{50}$ 値，RBA 値はある放射性化合物と標的タンパク質の結合に対する被験化合物の阻害曲線を作成して算出する．特に $K_i$ 値は阻害実験によって得られた解離定数であり，$K_D$ 値が既知の放射性化合物を用いて被験化合物の $IC_{50}$ 値を算出し，この $IC_{50}$ 値と，用いた放射性リガンドの濃度と $K_D$ 値を使用して Cheng-Prusoff 式[21] によって算出する．したがって $IC_{50}$ 値は放射性リガンドの種類と濃度によって変化するが，$K_i$ 値はこれらに影響されない．論文によって使用した動物や組織，膜標品の作成方法，pH，温度，インキュベーション時間などの実験条件が少しずつ異なるため，完全に一致する実験はほとんど存在しないが，理論的には受容体が同じならば異なる論文間でも $K_i$ 値を比較することが可能であり，飽和曲線から算出した $K_D$ 値と阻害曲線から算出した $K_i$ 値は，理論的に同じ値となるはずである．スクリーニングなどで一度に多数の化合物の解離定数を求めるときは，それら各化合物の

すべてを放射性同位元素で標識して飽和実験を行い $K_D$ 値を算出するよりも，特定の標識化合物と標的タンパク質の結合に対する結合阻害実験を行って $K_i$ 値を求める方が一般的であり，実際にこのようにして求めた親和性データは数多く報告されている．以上の理由から，*Ki*Bank では受容体結合親和性を示すデータとして $K_i$ 値を採用した．

受容体と化合物の相互作用データを蓄積したデータベースとして，既に CLiBE[22] や $K_i$ Database[23] が一般公開されている．また，商用データベースの1つで化合物の開発情報・特許情報を取り扱っている Integrity (Prous Science, Spain) にも同様のデータが含まれている．

これらはいずれも *Ki*Bank よりも先行しているためより多くのデータを蓄積しているが，受容体結合親和性データとして $IC_{50}$ 値を含んでいるばかりではなく，*in vivo* の生理活性データまでも多数含んでいる．このため，これらのデータベースを *in silico* スクリーニングの結果を検討する目的で使用する場合は，データの解釈や取捨選択といった煩雑な作業が必要となる．その点，*Ki*Bank は上述したように結合親和性のデータが $K_i$ 値に統一されているため，これらの作業は不要である．

*Ki*Bank の利用法として，われわれは次のような状況を想定している．

創薬の開始段階で標的タンパク質を決定したら，そのタンパク質に親和性を示すと報告されている化合物を *Ki*Bank で検索する．それらの化合物について，最近その実用性が示された非経験的フラグメント分子軌道法（*ab initio* Fragment Molecular Orbital 法）[24]などにより結合エネルギーを求め，文献上の $K_i$ 値との回帰直線を描いておく (Fig. 3(A))．次に，新たにデザインした化合物と標的タンパク質との結合エネルギーを計算し，回帰線から $K_i$ 値を推測する (Fig. 3(B))．$K_i$ 値が十分小さくなければ，すなわち親和性が十分大きくなければ分子修飾を行って，十分小さな $K_i$ 値が得られるまで同じ作業を繰り返す．こうして選択された少数の化合物の

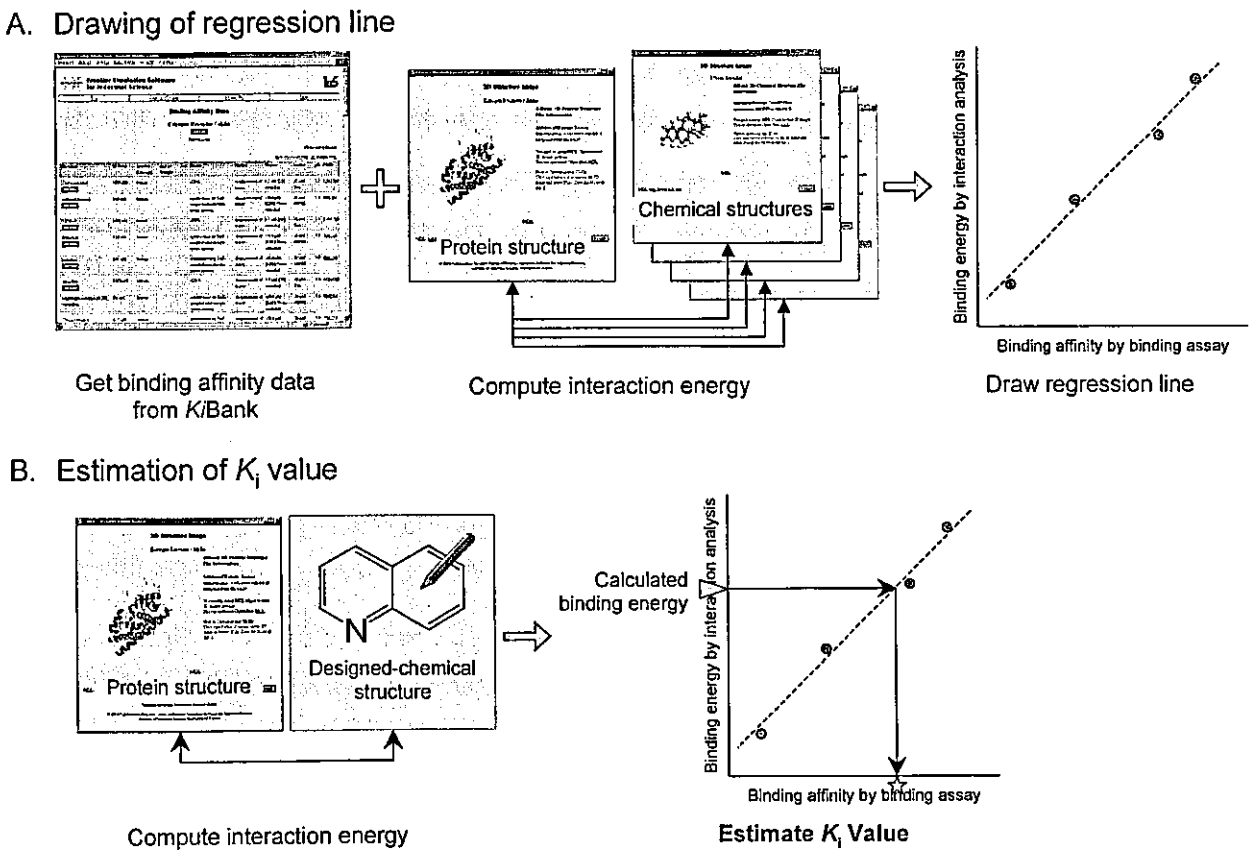


Fig. 3. A Schematic Diagram of an Application of *Ki*Bank for Structure-based Drug Design

Step 1: drawing regression line with binding affinity data from *Ki*Bank and results of protein-chemical interaction analysis (A). Step 2: estimating $K_i$ value from calculated binding energy (B).

みを実際に合成し，*in vitro* 又は *in vivo* のスクリーニングにかけて生理活性を試験する．コンピュータによるスクリーニングは24時間を通して行うことが可能なので，リード化合物を見い出すまでの時間と労力の大幅な削減が期待できる．

さらに，研究対象の化合物が標的タンパク質以外のタンパク質と親和性を示すかどうか，示すとすればどの程度の強さかを検討することによって，副作用の可能性を予測し，さらには既存薬物の持つ副作用の可能性を軽減する方向を検討することも可能になると思われる．また，*Ki*Bankには，医薬品として開発された化合物だけではなく，開発過程で脱落した化合物や親和性が極めて低い化合物も収載されている．これらの「ネガティブデータ」は，化合物の分子修飾の過程で貴重な情報源に成り得ると考えられる．さらに，骨格の異なる複数の化合物群が開発あるいは研究されている場合には，それらのデータを比較検討し，分子軌道計算の助けも借りて新しい骨格の設計にも寄与することが考えられる．

現在のところ，標的タンパク質の種類は膜受容体と核内受容体に限定されているが，今後，酵素，チャネル，トランスポーターなどの他の種類の標的タンパク質についても親和性情報を収集するとともに，化合物とタンパク質の三次元座標データの蓄積・基礎情報の収集を続け，相互作用解析のためのデータベースとして一層の充実を図る予定である．

謝辞　本研究は，文部科学省ITプログラム「戦略的基盤ソフトウェアの開発」において実施された．また，一部厚生労働科学研究費トキシコゲノミクスの支援を受けた．

## REFERENCES AND NOTES

1) Drews J., *Science*, **287**, 1960–1964 (2000).
2) National Center for Biotechnology Information, National Library of Medicine, NIH: http://www.ncbi.nlm.nih.gov/entrez/query.fcgi, PubMed, 26 March 2004.
3) Nakata K., *Front. Biosci.*, **7**, C68–C73 (2002).
4) Nakata K., Takai-Igarashi T., Nakano T., Kaminuma T., *Data Sci. J.*, **1**, 140–145 (2002).
5) Division of Safety Information on Drug, Food and Chemicals, NIHS: http://moldb.nihs.go.jp/jan/Default.htm, Japanese Accepted Names for Pharmaceuticals (JAN Database), 26 March 2004.
6) Halgren T. A., *J. Comput. Chem.*, 20, 720–729 (1999).
7) Berman H. M., Westbrook J., Feng Z., Gilliland G., Bhat T. N., Weissig H., Shindyalov I. N., Bourne P. E., *Nucleic Acids Res.*, **28**, 235–242 (2000).
8) Word J. M., Lovell S. C., Richardson J. S., Richardson D. C., *J. Mol. Biol.*, **285**, 1735–1747 (1999).
9) Cornell W. D., Cieplak P., Bayly C. I., Gould I. R., Merz K. M., Ferguson D. M., Spellmeyer D. C., Fox T., Caldwell J. W., Kollman P. A., *J. Am. Chem. Soc.*, **117**, 5179–5197 (1995).
10) Liang S., Grishin N. V., *Protein Sci.*, **11**, 322–331 (2002).
11) Xiang Z., Honig B., *J. Mol. Biol.*, **311**, 421–430 (2001).
12) Bower M. J., Cohen F. E., Dunbrack Jr., R. L., *J. Mol. Biol.*, **267**, 1268–1282 (1997).
13) Wu C. H., Yeh L. S., Huang H., Arminski L., Castro-Alvear J., Chen Y., Hu Z., Kourtesis P., Ledley R. S., Suzek B. E., Vinayaka C. R., Zhang J., Barker W. C., *Nucleic Acids Res.*, **31**, 345–347 (2003).
14) Boeckmann B., Bairoch A., Apweiler R., Blatter M. C., Estreicher A., Gasteiger E., Martin M. J., Michoud K., O'Donovan C., Phan I., Pilbout S., Schneider M., *Nucleic Acids Res.*, **31**, 365–370 (2003).
15) Benson D. A., Karsch-Mizrachi I., Lipman D. J., Ostell J., Wheeler D. L., *Nucleic Acids Res.*, **31**, 23–27 (2003).
16) Cuticchia A. J., *Hum. Mutat.*, **15**, 62–67 (2000).
17) Sherry S. T., Ward M. H., Kholodov M., Baker J., Phan L., Smigielski E. M., Sirotkin K., *Nucleic Acids Res.*, **29**, 308–311 (2001).
18) Hamosh A., Scott A. F., Amberger J., Bocchini C., Valle D., McKusick V. A., *Nucleic Acids Res.*, **30**, 52–55 (2002).
19) Matys V., Fricke E., Geffers R., Gossling E., Haubrock M., Hehl R., Hornischer K., Karas D., Kel A. E., Kel-Margoulis O. V., Kloos D. U., Land S., Lewicki-Potapov B., Michael H.,

Munch R., Reuter I., Rotert S., Saxel H., Scheer M., Thiele S., Wingender E., *Nucleic Acids Res.*, **31**, 374–378 (2003).
20) Altschul S. F., Madden T. L., Schäffer A. A., Zhang J., Zhang Z., Miller W., Lipman D. J., *Nucleic Acids Res.*, **25**, 3389–3402 (1997).
21) Cheng Y., Prusoff W. H., *Biochem. Pharmacol.*, **22**, 3099–3108 (1973).
22) Chen X., Ji Z. L., Zhi D. G., Chen Y. Z., *Comput. Chem.*, **26**, 661–666 (2002).
23) NIMH Psychoactive Drug Screening Program: http://kidb.bioc.cwru.edu/, $K_i$ Database, 26 March 2004.
24) Fukuzawa K., Kitaura K., Nakata K., Kaminuma T., Nakano T., *Pure Appl. Chem.*, **75**, 2405–2410 (2003).

ANALYTICAL SCIENCES APRIL 2004, VOL. 20



Notes

# Improvement in Reliability of Probabilistic Test of Significant Differences in GeneChip Experiments

**Kyoko TODA,[†] Seiichi ISHIDA,[†] Kotoko NAKATA, Rieko MATSUDA, Yukari SHIGEMOTO-MOGAMI, Shogo OZAWA, Jun-ichi SAWADA, Yasuo OHNO, Kazuhide INOUE, Koichi SHUDO, and Yuzuru HAYASHI[††]**

*National Institute of Health Sciences, 1-18-1 Kami-Yoga, Setagaya, Tokyo 158-8501, Japan*

A probabilistic test (FUMI theory) for GeneChip experiments has been proposed for selecting the genes which show significant differences in the gene expression levels between a single pair of treatment and control. This paper describes that the reliability of the judgment by the FUMI theory can be enhanced, when the selected genes are referred to biomolecular-functional networks of a commercial database. The genes judged as being differently expressed are grouped into a cluster in the biomolecular networks. It is also demonstrated that false positive genes have a trend in the networks to be isolated from each other, and also away from the clustered genes, since the false positive genes are randomly selected.

**(Received October 17, 2003; Accepted February 23, 2004)**

## Introduction

The GeneChip technology has recently made rapid progress, but some important problems still remain open. For example: 1) The GeneChips are expensive, and the replication of experiments is not easy; 2) The GeneChips generate tens of thousands of data for every experiment, and a new method for handling such voluminous data efficiently is desired.

In a previous paper,[1] we put forward a method for detecting significant changes between two different conditions from a single pair of experiments, that is, treatment and control. The method is called FUMI theory (FUnction of Mutual Information).[2,3] Under the condition of the paper, out of 12559 genes on the chip, 200 - 310 genes were selected as differently expressed with 1% risk. Due to the risk of 1%, however, 126 genes must be falsely selected. This number of false positive genes is critical compared to the totally selected genes (200 - 310).

The simplest solution to the problems will be to refer to the results of repeated experiments under the same conditions.[4] It is quite probable that the genes of true differences in the expression will be selected once and again by the replicates. On the other hand, the false positive genes will be selected at random, and not many times.

This paper proposes a method to make the judgment based on the FUMI theory more reliable, *i.e.*, a method to distinguish between the true positive and false positive, even from a single pair of treatment and control experiments. For this purpose, a commercially available database which provides a biomolecule-functional network is integrated.

## Experimental

The details of experiments for the microarray analysis were previously described.[1] Human promyelocytic leukemia cell line (HL60) cells were exposed to 20 nM 12-*O*-tetradecanoyl-phorbol 13-acetate (TPA) for 9 h and biotin-labeled cRNA was prepared and stored as a stock solution for later hybridization. A total of four GeneChip arrays (Human Genome U95A set, Affymetrix, Inc) were used for hybridization (two with the TPA-exposed stock solution and two with the control stock solution). One of four combinations of exposure and control experiments was taken as an example in the text. The others were used for reference.

The network of proteins (Fig. 1) was drawn with a commercial database (KeyMolnet, Institute of Medicinal Molecular Design Inc., Tokyo).

## Theory

In the FUMI theory, the *a priori* SD, $\sigma$, of microarray fluorescence measurements is described as a function of the averaged measurements, $X$:

$$\sigma = \sqrt{0.009636X^2 + 91897.8} \quad (1)$$

This relationship was obtained in our previous study from six replicate samples which were different from the target samples. Let $X_E$ be the expression level (measurement) of a gene for the exposed sample and $X_C$ be the measurement of the gene for the control sample. $\sigma$ is given by Eq. (1) as $X = |X_E + X_C|/2$. The judgment of the significant differences is performed based on the inequality:

$$\frac{|X_E - X_C|}{\sqrt{2}\sigma} > 2.58 \quad (2)$$

[†] Co-first authors.
[††] To whom correspondence should be addressed.
K. S. present address: Japan Pharmaceutical Information Center.

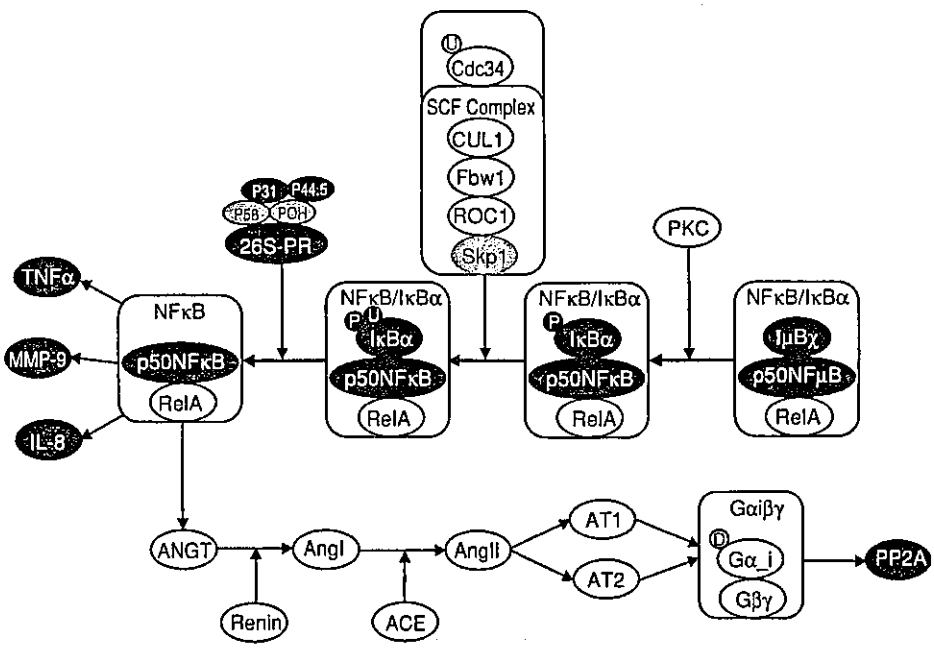


Fig. 1 Proteins with significant differences of gene expression. Significant differences with 1% risk (black background) and 5% risk (gray background) are judged by FUMI theory. The white background means no significant difference, except for PKC and ROC1 which are not included in the U95A array. The network of the proteins is provided by KeyMolnet. Cdc34: Cell Division Cycle 34; SCF: Skp1/Cull1/F-box;[9] 26S-PR: 26S Proteasome;[10,11] ANGT: Angiotensinogen; AngI: Angiotensin I; ACE: Angiotensin I converting enzyme; AngII: Angiotensin II; AT1: angiotensin II receptor type 1; AT2: Angiotensin II receptor type 2; Gαiβγ: heterotrimeric G Protein. The subunits are represented as αi, and βγ. D represents the GDP-binding form.

where 2.58 is the critical value for a significant level of 1% under the assumption that the distribution of $X_E - X_C$ is normal. If the risk is raised from 1% to 5%, the critical value becomes 1.96.

## Results and Discussion

The FUMI theory provided the judgment with 1% risk that out of 12559 genes on the U95A array, 1231 genes were differently expressed between the TPA treated HL60 cells and control cells. Figure 1 illustrates the well-known pathways around the TPA receptor, PKC (protein kinase C).[5] TPA is known to promote the transcription of IL-8 (interleukin 8), TNFα (tumor necrosis factor α), and MMP-9 (matrix metalloproteinase 9) through the transcription factor, NFκB (NF kappa B).[6] In the figure, the black and gray ellipses represent the molecules for which the gene expression levels were judged to increase with 1% and 5% risks, respectively. The white ellipses denote the molecules which were judged to be unaffected by TPA. The small circles show the protein modification by phosphorylation (P) and ubiquitination (U). The arrows show the biological influence from one molecule to another. The molecules which function as a complex are grouped by the square.

The results from the significance test for one pair of experimental data (one treatment and one control) are discussed below. The tests for three other pairs of data, obtained under the same conditions, are used for corroboration. The genes on the pathways to IL-8, TNFα and MMP-9 were also judged as being affected in the other three tests, but PP2A (Protein phosphatase 2A), was not, even when the risk was increased to 5%.

From the above results, it follows that the genes selected by every significance test, *e.g.*, the pathways to IL-8, TNFα and MMP-9, will have a high probability that the gene expression level is truly different between the treatment and control. In the protein network diagram, the selected proteins appear as a cluster.

Among the 1231 genes selected by the FUMI theory, some gene groups which are similar to the PKC cluster are also found when they are applied to protein networks, *e.g.*, EGR-1[7] and $p21^{Waf1/Cip1}$.[8] These genes are well-known to be induced by TPA,[7,8] and are involved in the 753 genes which were selected from each of the four pairs of exposure and control.

On the other hand, the isolated genes from the cluster, *e.g.*, PP2A, were selected only once from the four pairs. Therefore, PP2A was selected randomly, and can be concluded to be false positive. On the network, the false positive genes will be isolated from the clustered genes.

Among the selected 1231 genes, 97 genes were not selected by the other reference pairs of experiments, and are suspected to be false positive. They are all isolated from the PKC cluster. The number, 97, is close to the probable number of false positive genes when the risk is 1% (= 126). The number of genes suspected to be false positive is 80, 128, 129 for the reference pairs, respectively.

We can conclude that the combination of the test of significant difference (FUMI theory) with a protein network database (KeyMolnet) can substantially enhance the reliability of judgment. In other words, the true and false differences in the gene expression levels can be distinguished based on the relative position of the molecules in the protein network, *i.e.*, clustered or isolated. This paper has taken the well-known experiment as a model example, but the proposed method will

be applicable to practical problems.

The biological activities of the genes clustered in the database (KeyMolnet) can be confirmed, though not always, by literature. However, it will be quite difficult to find relevant papers on the isolated genes because of the randomness and abundance of their occurrence. Among 12559 genes, 1231 genes were selected by the FUMI theory as mentioned above. About 10000 genes can be candidates for the false positive on a gene chip and possibly only a part of these genes have been studied so far. Nevertheless, our purpose is to provide a method for estimating the unknown biological functions of the genes from the combination of insufficient information. The FUMI theory and database can play a complementary role in analyzing a huge amount of GeneChip data.

## Acknowledgements

We would like to thank Drs. Itai, Tomioka and Sato of the Institute of Medicinal Molecular Design, Inc. for their valuable suggestions and for kindly allowing us to use KeyMolnet. This work was supported in part by the Program for Promotion of Fundamental Studies in Health Sciences (MPJ-6 and MF-16) of the Organization for Pharmaceutical Safety and Research.

## References

1. K. Toda, S. Ishida, K. Nakata, R. Matsuda, Y. S. Mogami, K. Fujishita, S. Ozawa, J. Sawada, K. Inoue, K. Shudo, and Y. Hayashi, *Anal. Sci.*, **2003**, *19*, 1529.
2. Y. Hayashi and R. Matsuda, *Anal. Chem.*, **1994**, *66*, 2874.
3. R. Matsuda, Y. Hayashi, S. Sasaki, K. Saito, K. Iwaki, H. Harakawa, M. Satoh, Y. Ishizuki, and T. Kato, *Anal. Chem.*, **1998**, *70*, 319.
4. S. Ishida, E. Huang, H. Zuzan, R. Spang, G. Leone, M. West, and J. R. Nevins, *Mol. Cell Biol.*, **2001**, *21*, 4684.
5. S. J. Collins, *Blood*, **1987**, *70*, 1233.
6. H. L. Pahl, *Oncogene*, **1999**, *18*, 6853.
7. H. Q. Nguyen, B. Hoffman-Liebermann, and D. A. Liebermann, *Cell*, **1993**, *72*, 197.
8. V. Ullmannová, P. Stöckbauer, M. Hradcová, J. Souček, and C. Haškovec, *Leuk Res.*, **2003**, *27*, 1115.
9. K. Tanaka, T. Kawakami, K. Tateishi, H. Yashiroda, and T. Chiba, *Biochimie*, **2001**, *83*, 351.
10. O. Coux, K. Tanaka, and A. L. Goldberg, *Annu. Rev. Biochem.*, **1996**, *65*, 801.
11. V. Spataro, T. Toda, R. Craig, M. Seeger, W. Dubiel, A. L. Harris, and C. Norbury, *J. Biol. Chem.*, **1997**, *272*, 30470.

# A functional study on polymorphism of the ATP-binding cassette transporter ABCG2: critical role of arginine-482 in methotrexate transport

Hideyuki MITOMO*, Ryo KATO*, Akiko ITO†, Shiho KASAMATSU*, Yoji IKEGAMI†, Isao KII‡, Akira KUDO‡, Eiry KOBATAKE‡, Yasuhiro SUMINO§‖ and Toshihisa ISHIKAWA*[1]

*Department of Biomolecular Engineering, Graduate School of Bioscience and Biotechnology, Tokyo Institute of Technology, 4259 Nagatsuta, Midori-ku, Yokohama, 226-8501, Japan, †Department of Drug Metabolism and Disposition, Meiji Pharmaceutical University, Noshio 2-522-1, Kiyose-shi, Tokyo 204-8588, Japan, ‡Department of Biological Information, Graduate School of Bioscience and Biotechnology, Tokyo Institute of Technology, 4259 Nagatsuta, Midori-ku, Yokohama, 226-8501, Japan, §Strategic Product Planning Department, Takeda Chemical Industries, Ltd., 4-1-1 Doshomachi, Chuo-ku, Osaka 540-8645, Japan, and ‖Pharma SNP Consortium, The Japan Pharmaceutical Manufacturer's Association (JPMA), 3-4-1 Nihonbashihoncho, Chuo-ku, Tokyo 103-0023, Japan

Overexpression of the ATP-binding cassette transporter ABCG2 reportedly causes multidrug resistance, whereas altered drug-resistance profiles and substrate specificity are implicated for certain variant forms of ABCG2. At least three variant forms of ABCG2 have been hitherto documented on the basis of their amino acid moieties (i.e., arginine, glycine and threonine) at position 482. In the present study we have generated those ABCG2 variants by site-directed mutagenesis and expressed them in HEK-293 cells. Exogenous expression of the $Arg^{482}$, $Gly^{482}$, and $Thr^{482}$ variant forms of ABCG2 conferred HEK-293 cell resistance toward mitoxantrone 15-, 47- and 54-fold, respectively, as compared with mock-transfected HEK-293 cells. The transport activity of those variants was examined by using plasma-membrane vesicles prepared from ABCG2-overexpressing HEK-293 cells. [$Arg^{482}$]ABCG2 transports [$^3$H]methotrexate in an ATP-dependent manner; however, no transport activity was observed with the other variants ($Gly^{482}$ and $Thr^{482}$). Transport of methotrexate by [$Arg^{482}$]ABCG2 was significantly inhibited by mitoxantrone, doxorubicin and rhodamine 123, but not by *S*-octylglutathione. Furthermore, ABCG2 was found to exist in the plasma membrane as a homodimer bound via cysteinyl disulphide bond(s). Treatment with mercaptoethanol decreased its apparent molecular mass from 140 to 70 kDa. Nevertheless, ATP-dependent transport of methotrexate by [$Arg^{482}$]ABCG2 was little affected by such mercaptoethanol treatment. It is concluded that $Arg^{482}$ is a critical amino acid moiety in the substrate specificity and transport of ABCG2 for certain drugs, such as methotrexate.

Key words: ATP-binding cassette transporter (ABC transporter), ABCG2, acquired mutation, methotrexate, multidrug resistance, single nucleotide plymorphism.

## INTRODUCTION

Individual variations in response to a drug originate from different causes, such as genetic polymorphism and altered expression levels of drug target molecules (e.g. membrane receptors, nuclear receptors and enzymes), as well as those of drug-metabolizing enzymes and drug transporters [1]. To achieve the much-talked-about 'personalized medicine', it is critically important that we understand the molecular mechanisms and functions underlying such variations in drug response.

Cancer is one of the gene-associated diseases, with multiple factors involved in its cause and progression [2]. Despite enormous costs and efforts spent on the development of cancer chemotherapies, anticancer drugs are often effective only in a relatively small proportion of cancer patients. It has long been recognized that the effectiveness of anticancer drugs can vary significantly among individual patients. Indeed, acquired and intrinsic drug resistance in cancer is the major obstacle to long-term, sustained patient response to chemotherapy.

There is accumulating evidence that active export of anticancer drugs from cancer cells is one of the major mechanisms of drug resistance. Several ATP-binding cassette (ABC) transporters underlie multidrug resistance in cancer cells by actively extruding the clinically administered chemotherapeutic drugs. Two major ABC transporters, ABCB1 (P-glycoprotein or MDR1) and ABCC1 (MRP1), have been well studied in terms of their structure and function in cancer drug resistance [3–8]. In addition, a novel ABC transporter, breast-cancer-resistant protein (BCRP), has recently been discovered in doxorubicin-resistant breast-cancer cells [9]. The same transporter has also been found in human placenta [10] as well as in drug-resistant cancer cells selected by using mitoxantrone and DNA topoisomerase I inhibitors [11–18]. The newly found ABC transporter protein is now named ABCG2 and is classified in the G-subfamily of human ABC transporter genes according to the new nomenclature. ABCG is a so-called 'half-transporter' bearing six transmembrane domains and one ATP-binding cassette.

Overexpression of ABCG2 reportedly confers cancer-cell resistance to camptothecin-based anticancer drugs such as mitoxantrone, topotecan and 7-ethyl-10-hydroxycamptothecin (SN-38: active metabolite of irinotecan). SN-38-selected PC-6/SN2-5H human lung-carcinoma cells were shown to overexpress ABCG2 with the decreased intracellular accumulation of SN-38 and its glucuronide metabolite. We have recently demonstrated that plasma-membrane vesicles prepared from those cells ATP-dependently transported both SN-38 and SN-38-glucuronide, and our results strongly suggested that ABCG2 is involved in the active extrusion of SN-38 and its metabolite from cancer cells [19].

To date, at least three variant forms of ABCG2 have been documented on the basis of amino acid moieties at position 482, which is close to the third transmembrane domain. The wild-type

Abbreviations used: ABC, ATP-binding cassette; BCRP, breast-cancer-resistant protein; GAPDH, glyceraldehyde-3-phosphate dehydrogenase; HRP, horseradish peroxidase; MTT, bromo-3-(4,5-dimethyl-2-thiazoyl)-2,5-diphenyltetrazolium; RT, reverse transcription; SN-38, 7-ethyl-10-hydroxy-camptothecin; SNP, single-nucleotide polymorphism.

[1] To whom corrrespondence should be addressed (e-mail tishikaw@bio.titech.ac.jp).

form of ABCG2 has an arginine at that position [10], whereas other variants cloned from cancer cell lines [9,13] have glycine and threonine at position 482. It is currently speculated that the substrate specificities of ABCG2 may differ among those variant forms [18,20–22]. To elucidate the role of amino acid moieties at position 482 in the transport function, we have expressed each variant form of ABCG2 in HEK-293 cells and examined the substrate specificity of those variants. In the present study, we demonstrate that $Arg^{482}$ is critically involved in methotrexate transport mediated by ABCG2. Furthermore, we provide direct evidence that the ABCG2 protein functions as a homodimer bound via a cysteinyl disulphide bond(s).

## EXPERIMENTAL

### Cloning of human [$Arg^{482}$]ABCG2 cDNA

Human ABCG2 cDNA was cloned from mRNA of the MCF7/BCRP clone-8 cell line [9]. Briefly, reverse transcription (RT)-PCR was carried out by using the SuperScript First-Strand Synthesis System (Invitrogen, Carlsbad, CA, U.S.A.) and the following specific primers: sense 5′-CTCTCCAGATGTCTTCC-AGT-3′ and antisense 5′-ACAGTGTGATGGCAAGGGAAC-3′, where the primers were designed based on the ABCG2 cDNA sequences. The PCR reaction consisted of 30 cycles of 95 °C for 30 s, 58 °C for 30 s and 72 °C for 2 min, as previously described [23]. The resulting PCR product was inserted into the pCR2.1 TOPO vector (Invitrogen) and its sequences were analysed by automated DNA sequencing (TOYOBO Gene Analysis, Tokyo, Japan). The open reading frame of the ABCG2 cDNA, thus obtained, was identical with the ABCG2 wild-type ($Arg^{482}$) originally named ABCP (GenBank® accession number AF103796). The [$Arg^{482}$]ABCG2 cDNA was removed from the pCR2.1 TOPO vector by *Eco*RI digestion. After the treatment with alkaline phosphatase, the cDNA was ligated to the *Eco*RI sites of the pcDNA3.1 Expression vector (Invitrogen) using the Rapid DNA Ligation Kit (Roche Diagnosis Co., Indianapolis, IN, U.S.A.).

### Generation of variant forms by site-directed mutagenesis

The pcDNA3.1 vector carrying the [$Arg^{482}$]ABCG2 cDNA was used as the template, and variant forms ($Gly^{482}$ and $Thr^{482}$) were created by the site-directed mutagenesis using the QuikChange Site-directed Mutagensis Kit (Stratagene, La Jolla, CA, U.S.A.) and internal complementary PCR primers as follows: 5′-CT-GATTTATTACCCATGGGGATGTTACCAAGTATT-3′ and 5′-AATACTTGGTAACATCCCCATGGGTAATAAATCAG-3′ (for the $Gly^{482}$ variant form) or 5′-CTGATTTATTACCCATGACG-ATGTTACCAAGTATT-3′ and 5′-AATACTTGGTAACATCGT-CATGGGTAATAAATCAG-3′ (for the $Thr^{482}$ variant form). The PCR reaction consisted 16 cycles of 95 °C for 30 s, 55 °C for 1 min and 68 °C for 15 min, and *Pfu Turbo* DNA polymerase was used for the PCR reaction. The mutations were confirmed by sequencing the inserted cDNA.

### Cell culture

HEK-293 cells were maintained in Dulbecco's modified Eagle's medium supplemented with 10 % (v/v) heat-inactivated fetal-calf serum, penicillin (100 units/ml), and streptomycin (100 $\mu$g/ml) in a humidified atmosphere of 5 % $CO_2$ in air. The number of viable cells was determined in a haemocytometer by Trypan Blue dye exclusion.

**Table 1 Experimental conditions for quantitative PCR**

| | | | Denaturation | | PCR (45 cycles) | |
|---|---|---|---|---|---|---|
| Gene | Amplified position | Accession no. | Temp. (°C) | Time (s) | Temp. (°C) | Time (s) |
| ABCG2 | 2062–2287 | NM004827 | 95 | 30 | 95 | 15 |
| | | | | | 70 | 20 |
| | | | | | 82 | 7 |
| ABCC1 | 4436–4836 | NM004996 | 95 | 30 | 95 | 15 |
| | | | | | 68 | 20 |
| | | | | | 83 | 7 |
| ABCC2 | 3650–4029 | NM000392 | 95 | 30 | 95 | 15 |
| | | | | | 63 | 15 |
| | | | | | 72 | 15 |
| | | | | | 85 | 7 |
| ABCC3 | 4580–4890 | Y17151 | 95 | 30 | 95 | 15 |
| | | | | | 63 | 15 |
| | | | | | 72 | 15 |
| | | | | | 83 | 7 |
| ABCC4 | 2819–3129 | NM005845 | 95 | 30 | 95 | 15 |
| | | | | | 56 | 15 |
| | | | | | 72 | 15 |
| | | | | | 83 | 7 |
| ABCC5 | 4341–4572 | NM005688 | 95 | 30 | 95 | 15 |
| | | | | | 61 | 15 |
| | | | | | 72 | 15 |
| | | | | | 87 | 7 |
| GAPDH | 812–1130 | AF261085 | 95 | 30 | 95 | 15 |
| | | | | | 68 | 15 |
| | | | | | 89 | 7 |

HEK-293 cells were transfected with the pcDNA3.1 vector carrying the ABCG2 cDNA (see Figure 1A below) and the LIPOFECTAMINE™ reagent (Invitrogen) according to the manufacturer's instruction. Single colonies resistant to G418 (Nacalai Tesque, Kyoto, Japan) were picked and subcultured. Selection of positive colonies was performed by immunoblotting, as described below.

### Quantitative RT-PCR

Total RNA was extracted from cultured cells with the ISOGEN RNA extraction solution (WAKO Pure Chemical Industries, Ltd., Osaka, Japan) according to the manufacturer's protocol. cDNA was prepared from the extracted RNA in the reverse transcriptase reaction with SuperScript II RT (Invitrogen) and oligo(dT) primers according to the manufacturer's instructions. The transcriptome level of each ABC transporter was determined by quantitative PCR in a TaKaRa SmartCycler™ (TaKaRa Bio Inc., Shiga, Japan) with SYBR Green I (BioWhittaker Molecular Applications, Rockland, ME, U.S.A.) as a fluorescence indicator and the following specific primer sets for ABCG2, ABCC1, ABCC2, ABCC3, ABCC4, ABCC5 and glyceraldehyde-3-phosphate dehydrogenase (GAPDH): ABCG2 (5′-GATCTCTC-ACCCTGGGGCTTGTGGA, 5′-TGTGCAACAGTGTGATGG-CAAGGGA), ABCC1 (5′-GCCCTTCCTGACAAGCTAGAC, 5′-CATATAGGCCCTGCAGTTCTGAC), ABCC2 (5′-AGGTG-GCTTGCAATTCGCCT, 5′-CCAATCTTCTCCATGCTACCG-ATGT), ABCC3 (5′-CTAGAGGCATCTTCTACGGGA, 5′-ATA-ACACTCAGTTGGGAATCGG), ABCC4 (5′-TCCCACTTGTC-ATCTTCTCTC, 5′-CAGCACTTTGTCGAACACAC), ABCC5 (5′-GTGGAGTTTGACACCCCATCGGTC, 5′-CCAATCCGG-AACTGCTGTGCGAAAG), GAPDH (5′-ACTGCCAACGTGT-CAGTGGTGGACCTGA; 5′-GGCTGGTGGTCCAGGGGTCT-TACTCCTT). PCR conditions for the detection of these transporters and GAPDH are summarized in Table 1.

### Immunofluorescence microscopy

Mock- and ABCG2-transfected HEK-293 cells were seeded on microscopic cover glasses and incubated under the above-mentioned culture conditions overnight. Cells were fixed with 4% (w/v) paraformaldehyde in PBS at room temperature. Thereafter, cell membranes were permeabilized by incubating them with 0.1% Triton X-100 in PBS at room temperature for 5 min. Cells were then treated with the BXP-21 antibody (1:20 dilution; Signet Laboratories Inc., Dedham, MA, U.S.A.) as the first antibody and subsequently with the fluorescent-dye-Cy3-conjugated anti-mouse IgG antibody (1:500 dilution; Jackson ImmunoResearch Laboratories, Inc., Baltimore, MA, U.S.A.). The immunofluorescence of HEK-293 cells was detected with a confocal laser-scanning fluorescence microscope IX70/Fluoview (Olympus; Tokyo, Japan).

### Preparation of plasma-membrane vesicles from HEK-293 cells

HEK-293 cells (approx. $2 \times 10^9$ cells) were harvested by centrifugation and suspended in 100 ml of ice-cold PBS. After centrifugation at 500 *g* for 5 min, the cell pellet was diluted 40-fold with a hypotonic buffer [0.5 mM sodium phosphate (pH 7.0)/0.1 mM EGTA] and homogenized with a Potter–Elvehjem homogenizer. After centrifugation at 9100 *g*, the resulting supernatant was centrifuged at 100000 *g* for 30 min, and the resulting pellet was suspended in 250 mM sucrose containing 10 mM Tris/HCl, pH 7.4. The crude membrane fraction was layered over 38% (w/v) sucrose solution and centrifuged at 100000 *g* for 30 min. The turbid layer at the interface was collected, suspended in 250 mM sucrose containing 10 mM Tris/HCl, pH 7.4, and centrifuged at 100000 *g* for 30 min. The membrane fraction was collected and resuspended in a small volume (150–250 $\mu$l) of 250 mM sucrose containing 10 mM Tris/HCl, pH 7.4. After the measurement of protein concentration by the BCA (bicinchoninic acid) Protein Assay Kit (Pierce, Rockford, IL, U.S.A.), the membrane solution was stored at − 80 °C until used.

### Detection of ATP-dependent transport of [$^3$H]methotrexate

Frozen stocked membrane was thawed quickly at 37 °C, and vesicles were formed by passing the suspension through a 27-gauge needle. The standard incubation medium contained plasma-membrane vesicles (30 or 60 $\mu$g of protein), 500 $\mu$M [3′,5′,7′-$^3$H]methotrexate (Amersham Biosciences), 250 mM sucrose, 10 mM Tris/HCl, pH 7.4, 10 mM $MgCl_2$, 1 mM ATP, 10 mM creatine phosphate and 100 $\mu$g/ml creatine kinase in a final volume of 110 $\mu$l. The reaction was started by adding [$^3$H]methotrexate to the incubation medium. The reaction was carried out at 37 °C, and the amount of [$^3$H]methotrexate incorporated into the vesicles was measured by a rapid-filtration technique previously described [24].

### Gel electrophoresis and detection of ABCG2 protein

Expression of ABCG2 in HEK-293-cell membranes was determined by immunoblotting with BXP-21 (Signet), a specific antibody to human ABCG2 where membrane proteins were pretreated with or without mercaptoethanol (more details are given in the Results section). Briefly, proteins of the isolated plasma membrane were separated by electrophoresis on SDS/7.5%-(w/v)-polyacrylamide slab gels, and the proteins were electroblotted on to Hy-bond ECL® (enhanced chemiluminescence) nitrocellulose membranes (Amersham Biosciences). Immunoblotting was performed by using BXP-21 (1:250 dilution) as the first antibody and an anti-mouse IgG–horseradish peroxidase (HRP) conjugate (Cell Signaling Technology, Beverly, MA, U.S.A.) (1:3000 dilution) as the secondary antibody. HRP-dependent luminescence was developed by using Western Lighting Chemiluminescent Reagent Plus (PerkinElmer Life Sciences, Boston, MA, U.S.A.) and detected with a Lumino Imaging Analyzer FAS-1000 (Toyobo, Osaka, Japan).

### Profiling of drug resistance of ABCG2-overexpressing HEK-293 cells

A growth inhibition ($IC_{50}$) assay was performed by seeding HEK-293 cells at a density of 1000–2000 cells/well in 96-well plates containing the culture medium. After 24 h, mitoxantrone or methotrexate was added to the culture medium at different concentrations, and cells were further incubated with the drug in a humidified tissue-culture chamber (37 °C, 5% $CO_2$) for 72 h. Surviving cells were detected by the bromo-3-(4,5-dimethyl-2-thiazoyl)-2,5-diphenyltetrazolium (MTT) assay [25]. Briefly, 20 $\mu$l of MTT solution (5 mg/ml) was added to the culture medium, and cells were incubated for 4 h at 37 °C. Thereafter, the culture medium was removed and cells were dissolved in 200 $\mu$l of DMSO. The absorbance of formazan, a metabolite of MTT, in the resulting solution was photometrically measured at a test wavelength of 570 nm and at a reference wavelength of 630 nm in a Model 550 microplate reader (Bio-Rad, Hercules, CA, U.S.A.). $IC_{50}$ values were calculated from dose–response curves (i.e. cell survival versus drug concentration) obtained in multi-replicated experiments.

## RESULTS

### Expression of ABCG2 variants in HEK-293 cells

Three variant forms (i.e., $Arg^{482}$, $Gly^{482}$, and $Thr^{482}$) of human ABCG2 were expressed in HEK-293 cells by transfection with the pcDNA3.1 vector carrying the cDNA (Figure 1A). mRNA and protein levels of ABCG2 were detected by quantitative RT-PCR and Western blotting respectively; the mRNA levels of $Arg^{482}$, $Gly^{482}$ and $Thr^{482}$ variants in HEK-293 cells are shown in Figure 1(B). The parental HEK-293 cell line endogenously expressed ABCC1, ABCC2, ABCC4 and ABCC5, and the mRNA levels of ABCC3 and ABCG2 were below the detection limit. Similar expression profiles were observed in mock-transfected HEK-293 cells. On the other hand, in the $Arg^{482}$-, $Gly^{482}$- or $Thr^{482}$-variant-transfected cells, mRNA levels of ABCG2 were significantly enhanced, corresponding to 13–20% of the mRNA level of GAPDH. The expression levels of other ABC transporters, i.e., ABCC1, ABCC2, ABCC3, ABCC4 and ABCC5, were unchanged in these cells.

Western blotting (Figure 1C) revealed that the three variant forms of ABCG2 were also highly expressed at the protein level. In this experiment, membrane proteins were treated with mercaptoethanol prior to SDS/PAGE, so that one single band was detected with the BXP-21 antibody at an apparent molecular mass of 70 kDa. Mock-transfected HEK-293 cells, as the negative control, did not show any immunological reaction.

### Cellular localization of ABCG2 overexpressed in HEK-293 cells

Figure 2 depicts the differential interference (A and C) and immuno-fluorescence images (B and D) of mock- and [$Arg^{482}$]ABCG2-transfected HEK-293 cells. ABCG2 proteins

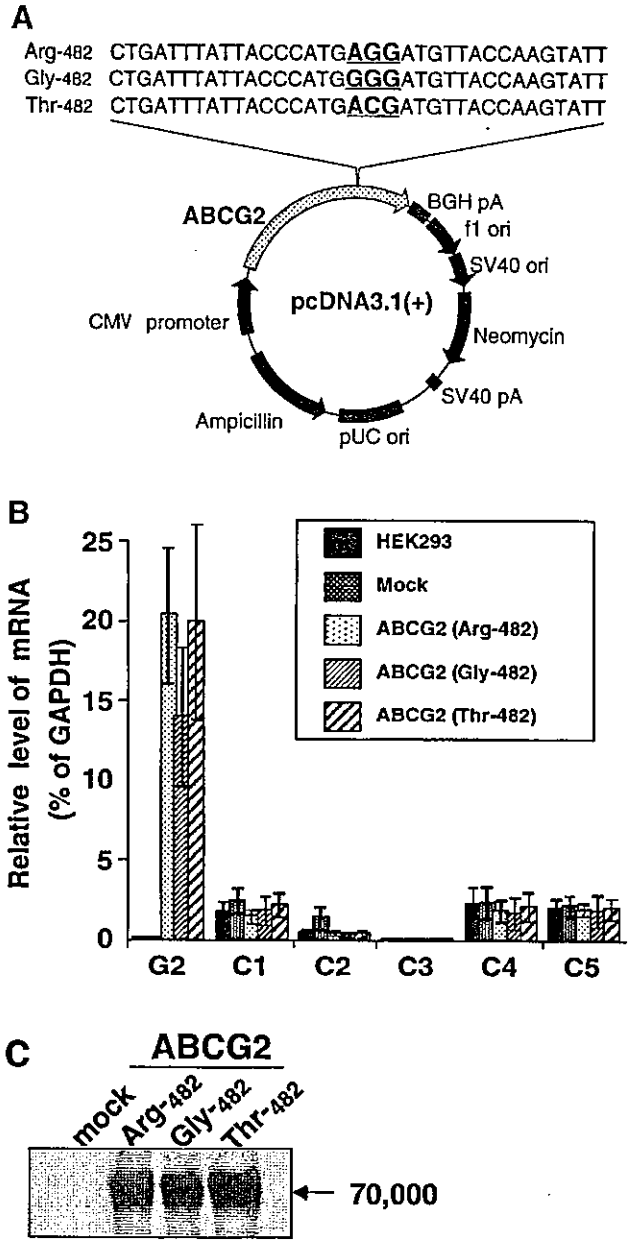


**Figure 1 Expression of ABCG2 variant forms in HEK-293 cells**

(**A**) Schematic illustration of the ABCG2 expression pcDNA3.1 vector. The partial cDNA sequences of three variants [$Arg^{482}$, $Gly^{482}$ and $Thr^{482}$ ('Arg-482' etc.)] are indicated. Abbreviations: BGH, bovine growth hormone; CMV, cytomegalovirus; f1ori, f1 origin of replication from the f1 filamentous phage; pA, polyadenylation sequence; pUC ori, pUC vector origin of replication; SV40, simian virus 40. (**B**) mRNA levels of ABCC1, ABCC2, ABCC3, ABCC4, ABCC5 and ABCG2 in mock- and [$Arg^{482}$]-, [$Gly^{482}$]- and [$Thr^{482}$]-ABCG2-transfected HEK-293 cells. Total RNA was extracted separately from those cells and cDNA was subsequently prepared by reverse transcriptase reaction. The transcriptome level of each ABC transporter was determined by quantitative PCR (for details, see the Experimental section). Data are expressed as means ± S.E.M. ($n = 4$). (**C**) Immunological detection of ABCG2 expressed in the plasma-membrane preparation from mock- and [$Arg^{482}$]-, [$Gly^{482}$]- or [$Thr^{482}$]-ABCG2-transfected HEK-293 cells. Membrane proteins (10 $\mu$g for each lane) were treated with mercaptoethanol prior to SDS/PAGE. Western blotting was performed as described in the Experimental section.

were probed with specific antibodies as described in the Experimental section. Strong immunofluorescence was detected at the plasma membrane of [$Arg^{482}$]ABCG2-transfected HEK-293 cells (Figure 2D). Similar results were obtained with HEK-293 cells expressing $Gly^{482}$ and $Thr^{482}$ variants as well

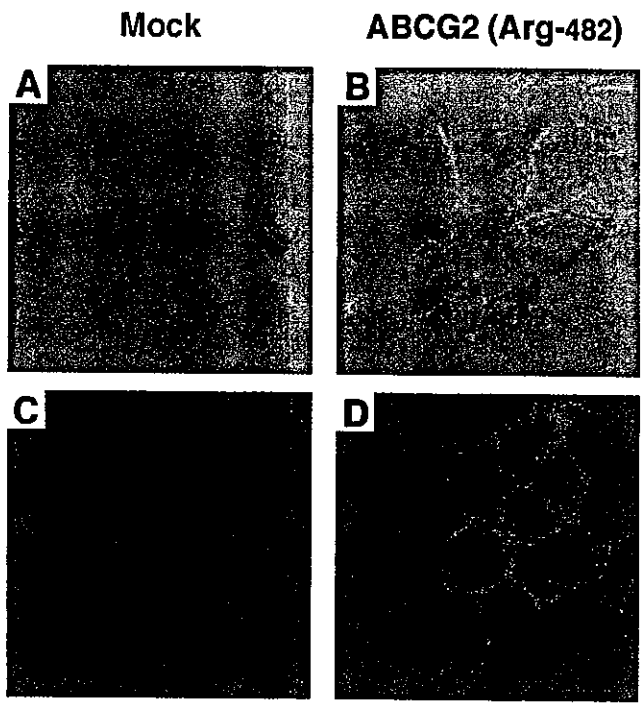


**Figure 2 Cellular localization of ABCG2 in HEK-293 cells**

Differential interference (**A**) and immunofluorescence (**B**) images of mock-transfected HEK-293 cells; differential interference (**C**) and immuno-fluorescence (**D**) images of [$Arg^{482}$]ABCG2-transfected HEK-293 cells. The ABCG2 protein was immunologically linked with the fluorescent Cy3 probe, as described in the Experimental section.

(results not shown). On the other hand, no immunofluorescence was detected in mock-transfected HEK-293 cells as the negative control (Figure 2B). Thus it is proven that those three ABCG2 variants were expressed predominantly in the plasma membrane of HEK-293 cells.

### Drug-resistant profile of ABCG2-transfected HEK-293 cells

Figure 3 shows the cellular resistance profiles of ABCG2-expressing HEK-293 cells to mitoxantrone and methotrexate. In this experiment, HEK-293 cells were incubated with mitoxantrone or methotrexate at different concentrations as indicated at 37 °C for 72 h. Overexpression of $Arg^{482}$, $Gly^{482}$ and $Thr^{482}$ variants conferred HEK-293 cells resistance to mitoxantrone by 15-, 47- and 54-fold respectively as compared with the mock-transfected HEK-293 cells (Figure 3A). The cellular resistance of $Gly^{482}$- or $Thr^{482}$-variant-expressing cells was even higher than that of $Arg^{482}$-variant-expressing cells. On the other hand, as shown in Figure 3(B), HEK-293 cells expressing $Arg^{482}$, $Gly^{482}$, and $Thr^{482}$ variants did not exhibit any significant resistance to methotrexate as compared with mock-transfected cells.

### ATP-dependent transport of methotrexate by [$Arg^{482}$]ABCG2

The function of $Arg^{482}$, $Gly^{482}$ and $Thr^{482}$ variants was examined by using plasma-membrane vesicles prepared from HEK-293 cells overexpressing those variants. Figure 4 depicts the time courses of methotrexate transport into plasma-membrane vesicles in the presence or absence of ATP. As previously described [24], the ATP concentration was maintained at constant levels for a period sufficient for measurement (at least 20 min) with the creatine

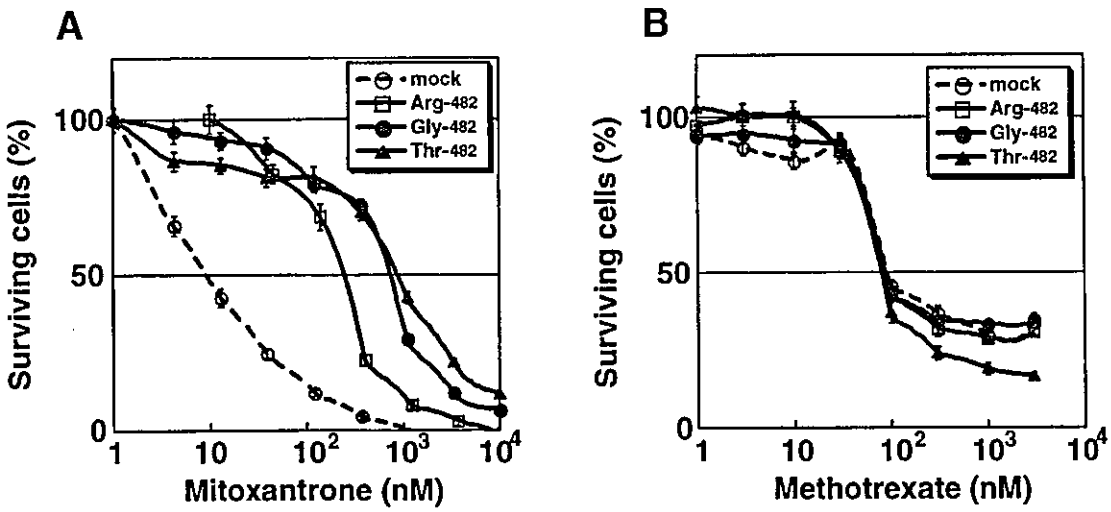


**Figure 3 Cellular resistance of ABCG2-expressing HEK-293 cells to mitoxantrone and methotrexate**

HEK-293 cells transfected with the mock vector or [$Arg^{482}$]-, [$Gly^{482}$]- and [$Thr^{482}$]-ABCG2 expression vectors were incubated in 200 $\mu$l of the culture medium containing mitoxantrone or methotrexate at different concentrations in 96-well plates in a humidified tissue-culture chamber (37 °C, 5 % $CO_2$). After 72 h, surviving cells were detected by the MTT assay (see the Experimental section). Data are expressed as means ± S.E.M. for multi-replicated ($n = 8$–12) experiments.

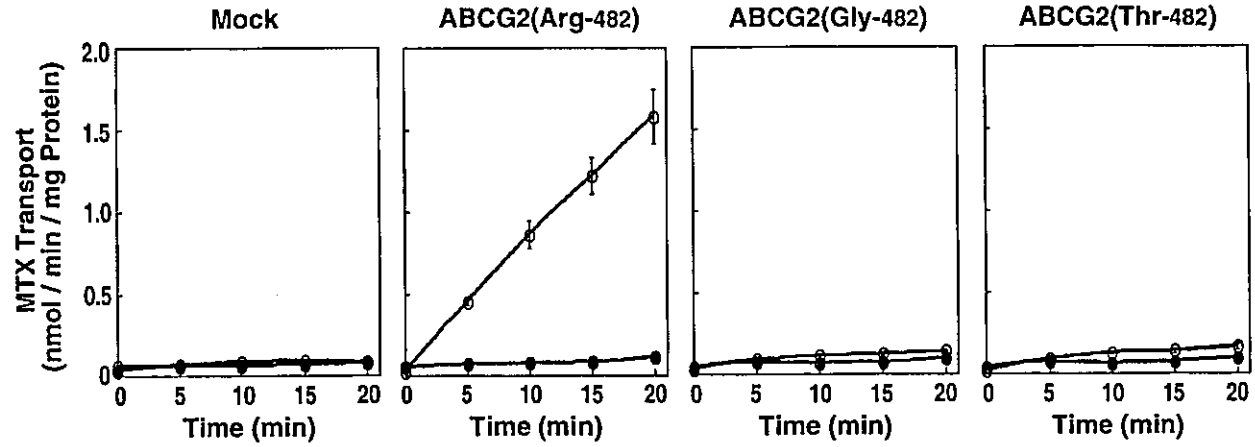


**Figure 4 ATP-dependent transport of methotrexate in plasma-membrane vesicles prepared from ABCG2-transfected HEK-293 cells**

Plasma-membrane vesicles were prepared from mock- and [$Arg^{482}$]-, [$Gly^{482}$]- or [$Thr^{482}$]-ABCG2-transfected HEK-293 cells as described in the Experimental section. Plasma-membrane vesicles (60 $\mu$g of protein) were incubated with 20 $\mu$M [$^3$H]methotrexate (MTX) in the absence (●) or presence (○) of 1 mM ATP in the medium containing 250 mM sucrose, 10 mM Tris/HCl, pH 7.4, 10 mM $MgCl_2$, 10 mM creatine phosphate and 100 $\mu$g/ml creatine kinase. The incubation was carried out at 37 °C and then stopped at different time points as indicated in the Figure. The amount of [$^3$H]methotrexate incorporated into the membrane vesicles was measured by a rapid-filtration technique. Results are expressed as means ± S.E.M. for triplicate experiments.

phosphate and creatine kinase reaction system. It is important to note that ATP-dependent methotrexate transport was observed only in plasma-membrane vesicles prepared from HEK-293 cells overexpressing the $Arg^{482}$ variant. No significant transport activity was detected from the $Gly^{482}$ or $Thr^{482}$ variant-expressing HEK-293 cells.

ATP-dependent transport of methotrexate by [$Arg^{482}$]ABCG2 was further characterized with the plasma-membrane-vesicle system. Figure 5(A) demonstrates a relationship between the methotrexate concentration and the rate of ATP-dependent transport. On the basis of this result, the apparent $K_m$ value for methotrexate was calculated to be 5.7 mM. In addition, as shown in Figure 5(B), ATP-dependent methotrexate transport mediated by [$Arg^{482}$]ABCG2 was inhibited by doxorubicin, mitoxantrone and rhodamine 123 at a concentration of 500 $\mu$M. In contrast, *S*-octylglutathione, which is a strong and competitive inhibitor for the GS-X (ATP-dependent glutathione-S-conjugate export) pump, e.g., ABCC1 and ABCC2 [24], had a minimal inhibitory effect (Figure 5B).

### Existence of ABCG2 as a homodimer in the plasma membrane

As shown in Figure 1(C), ABCG2 was detected as one single band at a molecular mass of 70 kDa under reducing conditions. On the other hand, without mercaptoethanol treatment, ABCG2 exhibited a molecular mass of 140 kDa. Figure 6(A) shows the effect of increasing concentrations of mercaptoethanol on the apparent molecular mass of [$Arg^{482}$]ABCG2. After a 20 min incubation with 100 mM mercaptoethanol at room temperature, the molecular mass of [$Arg^{482}$]ABCG2 completely

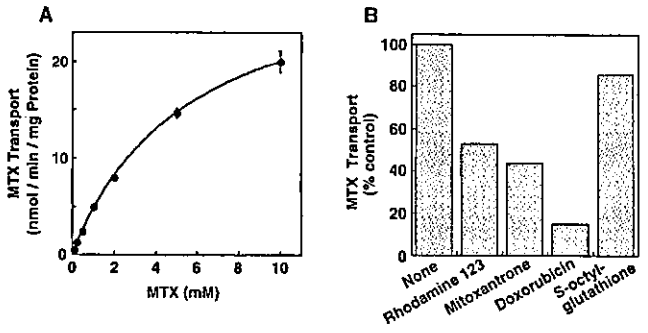


**Figure 5 Kinetic properties of ATP-dependent methotrexate transport by [Arg$^{482}$]ABCG2**

(A) Relationship between the methotrexate (MTX) concentration and the ATP-dependent MTX transport rate. Plasma-membrane vesicles (30 $\mu$g of protein) from [Arg$^{482}$]ABCG2-expressing HEK-293 cells were incubated with [$^3$H]methotrexate (MTX) at different concentrations (0–10 mM) in the incubation medium containing 1 mM ATP, 250 mM sucrose, 10 mM Tris/HCl, pH 7.4, 10 mM $MgCl_2$, 10 mM creatine phosphate and 100 $\mu$g/ml creatine kinase at 37 °C for 20 min. The amount of [$^3$H]methotrexate incorporated into the membrane vesicles was measured as shown in Figure 3. Data are expressed as means ± S.E.M ($n = 3$ for 0–0.5 mM; $n = 4$ for 1–10 mM). (B) Inhibition of ATP-dependent methotrexate transport by rhodamine 123, mitoxantrone, doxorubicin and *S*-octylglutathione. Plasma-membrane vesicles (30 $\mu$g of protein) were incubated with [$^3$H]methotrexate (500 $\mu$M) in the presence of those inhibitors (500 $\mu$M for each) in the incubation medium containing 1 mM ATP, 250 mM sucrose, 10 mM Tris/HCl, pH 7.4, 10 mM $MgCl_2$, 10 mM creatine phosphate and 100 $\mu$g/ml creatine kinase at 37 °C for 20 min. The amount of [$^3$H]methotrexate incorporated into the membrane vesicles was measured in the same manner. Data are normalized for the amount of [$^3$H]methotrexate incorporated during the incubation in the absence of inhibitors.

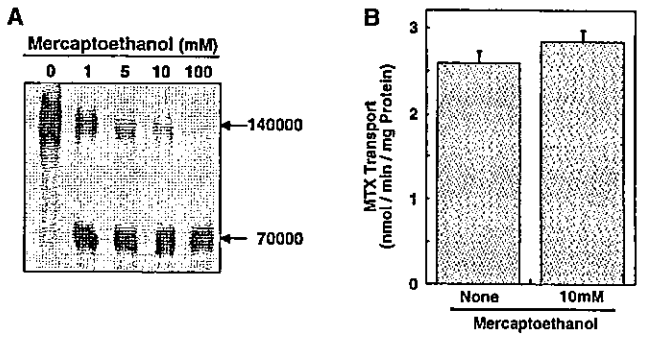


**Figure 6 Effect of mercaptoethanol on dimerization of ABCG2 (A) and ATP-dependent methotrexate transport (B)**

(A) The plasma membrane from [Arg$^{482}$]ABCG2-transfected HEK-293 cells was incubated with mercaptoethanol at final concentrations of 0, 1, 5, 10 and 100 mM in the medium containing 250 mM sucrose and 10 mM Tris/HCl, pH 7.4, at room temperature for 20 min. Thereafter, membrane proteins (2 $\mu$g for each lane) were separated by SDS/PAGE, and ABCG2 was immunologically detected by Western blotting, as shown in Figure 1(C). (B) The plasma membrane from [Arg$^{482}$]ABCG2-transfected HEK-293 cells was pre-incubated in the absence or presence of 10 mM mercaptoethanol at room temperature for 20 min, as described above. ATP-dependent methotrexate (MTX) transport was detected in the plasma-membrane vesicles as described in the Experimental section; the transport reaction was performed at 37 °C for 20 min. Data are expressed as means ± S.E.M. for triplicate experiments.

shifted to 70 kDa on Western-blotting analysis (Figure 6A). This phenomenon was not unique for the Arg$^{482}$ variant, since similar molecular-mass shifts were observed for the Gly$^{482}$ and Thr$^{482}$ variants as well (results not shown). These results suggest that ABCG2 exists in the plasma membrane as a homodimer bound through cysteinyl disulphide bond(s). It is noteworthy that ATP-dependent methotrexate transport was little affected by mercaptoethanol treatment, in spite of the breakage of the inter-peptide disulphide bonds (Figure 6B).

## DISCUSSION

### ATP-dependent methotrexate transport by [Arg$^{482}$]ABCG2

In the present study, we have established HEK-293 cell lines that overexpress three variant forms of human ABCG2 (Figures 1 and 2). Using the plasma-membrane vesicles prepared from those cells, we clearly demonstrate that [Arg$^{482}$]ABCG2 transports methotrexate; however, the other variants, Gly$^{482}$ and Thr$^{482}$, do not (Figure 4). The present study is the first report providing direct evidence that ABCG2 is able to transport methotrexate. Our finding strongly suggests that the Arg$^{482}$ close to the third transmembrane domain is a critical amino acid residue involved in the substrate specificity of ABCG2. Since the arginine residue is positively charged under physiological conditions, it is likely that its positive charge is a prerequisite for interactions between the active site of ABCG2 and anionic substrates such as methotrexate. However, as indicated by the weak inhibition by *S*-octylglutathione (Figure 5B), structural factors may also be important for the substrate recognition besides the negative charge. In fact, methotrexate transport was much more strongly inhibited by the glutathione conjugate of mitomycin C than by S-octylglutathione (H. Mitomo and T. Ishikawa, unpublished work).

Previous studies [26,27] have predicted the existence of energy-dependent transport systems for the methotrexate efflux from cells. Molecular cloning and functional expression of ABC transporters led to the identification of human ABCC1, ABCC2, ABCC3 and ABCC4 as methotrexate transporters [28–30]. These transporters belong to the C-subfamily of human ABC transporters and exhibit broad spectra of substrate specificity towards organic anions, including glutathione, glucuronide and sulphate conjugates, as well as nucleotide analogues [7,8]. The $K_m$ values for these ABC transporters in respect of methotrexate were reportedly in the range 200–500 $\mu$M [28–30]. Whereas HEK-293 cells endogenously express ABCC1, ABCC2, ABCC4 and ABCC5 (Figure 1B), ABCG2 expression was predominantly enhanced by transfection with the exogenous cDNA (Figures 1B and 1C). ABCG2 proteins were localized at the plasma membrane of HEK-293 cells (Figure 2). The $K_m$ value of ATP-dependent transport by [Arg$^{482}$]ABCG2 was estimated to be 5.7 mM for methotrexate (Figure 5A), approximately one order of magnitude greater than those reported for the above-mentioned ABCC-subfamily transporters.

### Variant forms of ABCG2 and drug-resistance phenotypes

Recently, Volk et al. [22] suggested that overexpression of the wild-type ([Arg482]ABCG2) mediates methotrexate resistance. Since the mitoxantrone-selected MCF7/MX cell line was used in their study, actual molecular mechanisms underlying the cross-resistance to mitoxantrone and methotrexate were not known. Our present study on ATP-dependent methotrexate transport mediated by [Arg$^{482}$]ABCG2 in part supports their hypothesis. Indeed, HEK-293 cells transfected with [Arg$^{482}$]ABCG2 were resistant to mitoxantrone (Figure 3A). However, [Arg$^{482}$]ABCG2-transfected cells did not exhibit significant resistance to methotrexate (Figure 3B). This may be explained by the high $K_m$ value (5.7 mM) of [Arg$^{482}$]ABCG2 in respect of methotrexate (Figure 5A). In addition, it is also true that the Arg$^{482}$-variant-transfected cells grew approx. 20% more slowly than the Gly$^{482}$- and Thr$^{482}$-variant-transfected cells, suggesting that overexpression of ABCG2 could result in an enhanced efflux of unknown, but physiologically important, substances from cells.

Until now, several acquired mutations were documented for ABCG2 cloned from drug-resistant cell lines [20,31]. Drug-resistant phenotypes vary among different cell lines expressing

variant types of ABCG2. In fact, transfectants with the wild-type ($Arg^{482}$) were not resistant to topotecan [18], whereas overexpression of the $Gly^{482}$ and $Thr^{482}$ variants conferred resistance to mitoxantrone, doxorubicin, daunorubicin and various camptothecin analogues, including topotecan [9,14–16]. Furthermore, $Gly^{482}$ and $Thr^{482}$ variants mediated the efflux of rhodamine 123 and doxorubicin from cells; however, $Arg^{482}$ did not [20,21]. These findings strongly suggest that arginine at position 482 has a critical role in the substrate specificity of ABCG2. The identification of mutations at 482 in ABCG2 may explain some discrepancies observed in the cross-resistance profiles of human cancer-cell lines. Likewise, one mutation 'hot spot' was identified at the same amino acid position 482 in mouse Abcg2 [32]. In the case of mouse Abcg2, variants of arginine, serine and methionine significantly affect the drug-resistance profile in cancer-cell lines [32].

To examine the function of ABCG2 as a drug transporter, we have previously established ABCG2-overexpressing Sf9 [fall armyworm (*Spodoptera frugiperda*)] insect cells and tried to measure drug-induced ATPase activity [23]. However, because of a high activity of endogenous ATPase present in the plasma membrane, we were not able to accurately measure the drug-induced ATPase activity of ABCG2 [23]. Özvegy et al. [21] had a similar difficulty in the case of the [$Arg^{482}$]ABCG2. In this context, the vesicle transport system we used in the present study may offer a simple and practical tool to elucidate the substrate specificity and transport activity of human ABCG2 and its variants.

## Homodimer formation of ABCG2

Since ABCG2 is an ABC half-transporter, it has been suspected that ABCG2 functions as a homodimer or heterodimer [15]. Most recently, using cross-linking reagents and specific antibodies, Litman et al. [33] provided evidence for the formation of an ABCG2 homodimer. In addition, Kage et al. [34] have recently established PA317 transfectants expressing c-Myc oncoprotein (Myc)- and haemagglutinin (HA)-epitope-tagged ABCG2 proteins, and they demonstrated that those hybrid proteins formed S–S homodimers. In the present study, by expressing native ABCG2 (without tag) in HEK-293 cells, we could provide more direct evidence that human ABCG2 exists in the plasma membrane as a homodimer bound through cysteinyl disulphide bond(s) (Figure 6). Treatment with mercaptoethanol decreased the apparent molecular mass of ABCG2 from 140 to 70 kDa (Figure 6A). It is noteworthy that ATP-dependent transport of methotrexate by [$Arg^{482}$]ABCG2 was little affected by mercaptoethanol treatment (Figure 6B). Thus disulphide-bond formation does not appear to be required for the transport function of ABCG2.

On the basis of the cDNA sequence, a total of 12 cysteine residues exist in the ABCG2 peptide. From a biochemical point of view, it may be interesting to study which cysteine residues participate in the disulphide-bond formation and how inter-peptide disulphide bonds are formed in the cell. Furthermore, ABCG1, ABCG4, ABCG5 and ABCG8 have been hitherto identified as ABC half-transporters [35], and it would be of interest to know whether those half-transporters also form homodimers or heterodimers via disulphide bonds as does ABCG2.

## Concluding remarks

ABCG2 is expressed in human normal tissues such as placental syncytiotrophoblasts, the epithelium of the small intestine and colon, the liver canalicular membrane, and ducts and lobules of the breast [36]. In addition, expression of ABCG2 is detected in venous and capillary endothelium [36]. Furthermore, relatively high expression of ABCG2 is observed in approx. 30% of acute-myeloid-leukaemia patients [37] and is correlated with an immature immunophenotype as determined by expression of the surface marker CD34 [38]. Not only expression levels, but also intrinsic genetic polymorphisms and acquired mutations of ABCG2, are suggested to affect the pharmacokinetic profile of drugs and thereby lead to individual variations in the drug response. Recently, two single-nucleotide polymorphisms (SNPs) leading to amino acid substitutions (i.e., $Val^{12} \rightarrow$ Met and $Gln^{141} \rightarrow$ Lys) for ABCG2 have been found in the Japanese population [39]. It is critically important to validate such SNPs and mutations by examining the actual function of the resulting gene products.

We thank Dr Masakazu Mie and Ms. Maki Kotaka for their helpful advice in performing the immunofluorescence microscopy. The present study was supported by research grants entitled 'Studies on the genetic polymorphism and function of pharmacokinetics-related proteins in the Japanese population' (H12-Genome-026) and 'Toxicoproteomics: expression of ABC transporter genes and drug–drug interactions' (H14-Toxico-002) from the Japanese Ministry of Health and Welfare as well as by a Grant-in-Aid for Creative Scientific Research (No. 13NP0401) and a research grant (No. 14370754) from the Japan Society for the Promotion of Science. In addition, this study was supported, in part, by the institutional core grant of the 21st Century COE (Centre of Excellence) Programme, the Ministry of Education, Culture, Sports, Science and Technology.

## REFERENCES

1 Kalow, W., Meyer, U. A. and Tyndale, R. F. (eds.) (2001) Pharmacogenomics, Marcel Dekker, New York
2 Hesketh, R. (1994) The Oncogene Handbook, Academic Press, London
3 Ling, V. (1997) Multidrug resistance: molecular mechanisms and clinical relevance. Cancer Chemother. Pharmacol. **40**, S3–S8
4 Ambudkar, S. V., Dey, S., Hrycyna, C. A., Ramachandra, M., Pastan, I. and Gottesman, M. M. (1999) Biochemical, cellular, and pharmacological aspects of the multidrug transporter. Annu. Rev. Pharmacol. Toxicol. **39**, 361–398
5 Klein, I., Sarkadi, B. and Váradi, A. (1999) An inventory of the human ABC proteins. Biochim. Biophys. Acta **1461**, 237–262
6 Dean, M., Rzhetsky, A. and Allikmets, R. (2001) The human ATP-binding cassette (ABC) transporter superfamily. Genome Res. **11**, 1156–1166
7 Borst, P. and Oude Elferink, R. (2002) Mammalian ABC transporters in health and disease. Annu. Rev. Biochem. **71**, 537–592
8 Ishikawa, T. (2003) Multidrug resistance in cancer: genetics of ABC transporters. In Nature Encyclopedia of the Human Genome (Cooper, D.N., ed.), vol. 4, pp. 154–160, Nature Publishing Group, London, in the press
9 Doyle, L. A., Yang, W., Abruzzo, L. V., Krogmann, T., Gao, Y., Rishi, A. K. and Ross, D. D. (1998) A multidrug resistance transporter from human MCF-7 breast cancer cells. Proc. Natl. Acad. Sci. U.S.A. **95**, 15665–15670
10 Allikmets, R., Schriml, L. M., Hutchinson, A., Romano-Spica, V. and Dean, M. (1998) A human placenta-specific ATP-binding cassette gene (ABCP) on chromosome 4q22 that is involved in multidrug resistance. Cancer Res. **58**, 5337–5339
11 Hazlehurst, L. A., Foley, N. E., Gleason-Guzman, M. C., Hacker, M. P., Cress, A. E., Greenberger, L. W., de Jong, M. C. and Dalton, W. S. (1999) Multiple mechanisms confer drug resistance to mitoxantrone in the human 8226 myeloma cell line. Cancer Res. **59**, 1021–1028
12 Rabindran, S. K., He, H., Singh, M., Brown, E., Collins, K. I., Annable, T. and Greenberger, L. M. (1998) Reversal of a novel multidrug resistance mechanism in human colon carcinoma cells by fumitremorgin C. Cancer Res. **58**, 5850–5858
13 Miyake, K., Mickley, L., Litman, T., Zhan, Z., Robey, R., Cristensen, B., Brangi, M., Greenberger, L., Dean, M., Fojo, T. and Bates, S. E. (1999) Molecular cloning of cDNAs which are highly overexpressed in mitoxantrone-resistant cells: demonstration of homology to ABC transport genes. Cancer Res. **59**, 8–13
14 Maliepaard, M., van Gastelen, M. A., de Jong, L. A., Pluim, D., van Waardenburg, R. C. A. M., Ruevekamp-Helmers, M. C., Floot, B. G. J. and Schellens, J. H. M. (1999) Overexpression of the BCRP/MXR/ABCP gene in a topotecan-selected ovarian tumor cell line. Cancer Res. **59**, 4559–4563

15 Ross, D. D., Yang, W., Abruzzo, L. V., Dalton, W. S., Schneider, E., Lage, H., Dietel, M., Greenberger, L., Cole, S. P. C. and Doyle, L. A. (1999) Atypical multidrug resistance: breast cancer resistance protein messenger RNA expression in mitoxantrone-selected cell lines. J. Natl. Cancer Inst. **91**, 429–433
16 Brangi, M., Litman, T., Ciotti, M., Nishiyama, K., Kohlhagen, G., Takimoto, C., Robey, R., Pommier, Y., Fojo, T. and Bates, S. E. (1999) Camptothecin resistance: role of the ATP-binding cassette (ABC), mitoxantrone-resistance half-transporter (MXR), and potential for glucuronidation in MXR-expressing cells. Cancer Res. **59**, 5938–5946
17 Litman, T., Brangi, M., Hudson, E., Fetsch, P., Abati, A., Ross, D. D., Miyake, K., Resau, J. H. and Bates, S. E. (2000) The multidrug-resistant phenotype associated with overexpression of the new ABC half-transporter, MXR (ABCG2). J. Cell Sci. **113**, 2011–2021
18 Nakagawa, R., Hara, Y., Arakawa, H., Nishimura, S. and Komatani, H. (2002) ABCG2 confers resistance to indolocarbazole compounds by ATP-dependent transport. Biochem. Biophys. Res. Commun. **299**, 669–675
19 Nakatomi, K., Yoshikawa, M., Oka, M., Ikegami, Y., Hayasaka, S., Sano, K., Shiozawa, K., Kawabata, S., Soda, H., Ishikawa, T. et al. (2001) Transport of 7-ethyl-10-hydroxycamptothecin (SN-38) by breast cancer resistance protein ABCG2 in human lung cancer cells. Biochem. Biophys. Res. Commun. **288**, 827–832
20 Honjo, Y., Hrycyna, C. A., Yan, Q.-W., Medina-Pérez, W. Y., Robey, R. W., van de Laar, A., Litman, T., Dean, M. and Bates, S. E. (2001) Acquired mutations in the MXR/BCRP/ABCP gene alter substrate specificity in MXR/BCRP/ABCP-overexpressing cells. Cancer Res. **61**, 6635–6639
21 Özvegy, C., Varadi, A. and Sarkadi, B. (2002) Characterization of drug transport, ATP hydrolysis, and nucleotide trapping by the human ABCG2 multidrug transporter. J. Biol. Chem. **277**, 47980–47990
22 Volk, E. L., Farley, K. M., Wu, Y., Li, F., Robey, R. W. and Schneider, E. (2002) Overexpression of wild-type breast cancer resistance protein mediates methotrexate resistance. Cancer Res. **62**, 5035–5040
23 Yoshikawa, M., Kasamatsu, S., Yasunaga, M., Wang, G., Ikegami, Y., Yoshida, H., Tarui, S., Yabuuchi, H. and Ishikawa, T. (2002) Does ABCG2 need a heterodimer partner? Expression and functional evaluation of ABCG2 (Arg-482). Drug Metab. Pharmacokin. **17**, 130–135
24 Ishikawa, T. (1989) ATP/$Mg^{2+}$-dependent cardiac transport system for glutathione S-conjugates: A study using rat heart sarcolemma vesicles. J. Biol. Chem. **264**, 17343–17348
25 Mosmann, T. (1983) Rapid colorimetric assay for cellular growth and survival: application to proliferation and cytotoxicity assays. J. Immunol. Methods **65**, 55–63
26 Schlemmer, S. R. and Sirotnak, F. M. (1992) Energy-dependent efflux of methotrexate in L1210 leukemia cells: evidence for the role of an ATPase obtained with inside-out plasma membrane vesicles. J. Biol. Chem. **267**, 14746–14752
27 Saxena, M. and Henderson, G. B. (1996) Identification of efflux systems for large anions and anionic conjugates as the mediators of methotrexate efflux in L1210 cells. Biochem. Pharmacol. **51**, 974–982
28 Hooijberg, J. H., Broxterman, H. J., Kool, M., Assaraf, Y. G., Peters, G. J., Noordhuis, P., Scheper, R. J., Borst, P., Pinedo, H. M. and Jansen, G. (1999) Antifolate resistance mediated by the multidrug resistance proteins MRP1 and MRP2. Cancer Res. **59**, 2532–2535
29 Kool, M., van der Linden, M., de Haas, M., Scheffer, G. L., de Vree, J. M., Smith, A. J., Jansen, G., Peters, G. J., Ponne, N., Scheper R. J. et al. (1999) MRP3, an organic anion transporter able to transport anti-cancer drugs. Proc. Natl. Acad. Sci. U.S.A. **96**, 6914–6919
30 Chen, Z.-S., Lee, K., Walther, S., Raftogianis, R. B., Kuwano, M., Zeng, H. and Kruh, G. D. (2002) Analysis of methotrexate and folate transport by multidrug resistance protein 4 (ABCC4): MRP4 is a component of the methotrexate efflux system. Cancer Res. **62**, 3144–3150
31 Komatani, H., Kotani, H., Hara, Y., Nakagawa, R., Matsumoto, M., Arakawa, H. and Nishimura, S. (2001) Identification of breast cancer resistant protein/mitoxantrone resistance/placenta-specific, ATP-binding cassette transporter as a transporter of NB-506 and J-107088, topoisomerase I inhibitors with an indolocarbazole structure. Cancer Res. **61**, 2827–2832
32 Allen, J. D., Jackson, S. C. and Schinkel, A. H. (2002) A mutation hot spot in the Bcrp1 (Abcg2) multidrug transporter in mouse cell lines selected for doxorubicin resistance. Cancer Res. **62**, 2294–2299
33 Litman, T., Jensen, U., Hansen, A., Covitz, K.-M., Zhan, Z., Fetsch, P., Abati, A., Hansen, P. R., Horn, T., Skovsgaad, T. and Bates, S. E. (2002) Use of peptide antibodies to probe for the mitoxantrone resistance-associated protein MXR/BCRP/ABCP/ABCG2. Biochim. Biophys. Acta **1565**, 6–16
34 Kage, K., Tsukahara, S., Sugiyama, T., Asada, S., Ishikawa, E., Tsuruo, T. and Sugimoto, Y. (2002) Dominant-negative inhibition of breast cancer resistance protein as drug efflux pump through the inhibition of S–S dependent homodimerization. Int. J. Cancer **97**, 626–630
35 Schmitz, G., Langmann, T. and Heimerl, S. (2001) Role of ABCG1 and other ABCG family members in lipid metabolism. J. Lipid Res. **42**, 1513–1520
36 Maliepaard, M., Scheffer, G. L., Faneyte, I. F., van Gastelen, M. A., Pijnenborg, A. C. L. M., Schinkel, A. H., van de Vijver, M. J., Scheper, R. J. and Schellens, J. H. M. (2001) Subcellular localization and distribution of the breast cancer resistance protein transporter in normal human tissues. Cancer Res. **61**, 3458–3464
37 Ross, D. D. (2000) Novel mechanisms of drug resistance in leukemia. Leukemia **14**, 467–473
38 van der Kolk, D. M., Vellenga, E., Scheffer, G. L., Müller, M., Bates, S. E., Scheper, R. J. and de Vries, E. G. E. (2002) Expression and activity of breast cancer resistance protein (BCRP) in *de novo* and relapsed acute myeloid leukemia. Blood **99**, 3763–3770
39 Iida, A., Saito, S., Sekine, A., Mishima, C., Kitamura, Y., Kondo, K., Harigae, S., Osawa, S. and Nakamura, Y. (2002) Catalog of 605 single-nucleotide polymorphisms (SNPs) among 13 genes encoding human ATP-binding cassette transporters: ABCA4, ABCA7, ABCA8, ABCD1, ABCD3, ABCD4, ABCE1, ABCF1, ABCG1, ABCG2, ABCG4, ABCG5, and ABCG8. J. Hum. Genet. **47**, 285–310

Received 22 January 2003/22 April 2003; accepted 13 May 2003
Published as BJ Immediate Publication 13 May 2003, DOI 10.1042/BJ20030150

Available online at www.sciencedirect.com
SCIENCE DIRECT®
Gene 310 (2003) 17–28
GENE
AN INTERNATIONAL JOURNAL ON GENES AND GENOMES
www.elsevier.com/locate/gene

# Characterization of the mouse *Abcc12* gene and its transcript encoding an ATP-binding cassette transporter, an orthologue of human ABCC12☆

Hidetada Shimizu[a], Hirokazu Taniguchi[b], Yoshitaka Hippo[b], Yoshihide Hayashizaki[c], Hiroyuki Aburatani[b], Toshihisa Ishikawa[a,*]

[a]*Department of Biomolecular Engineering, Graduate School of Bioscience and Biotechnology, Tokyo Institute of Technology, Nagatsuta 4259, Midori-ku, Yokohama 226-8501, Japan*
[b]*Genome Science Division, Research Center for Advanced Science and Technology, The University of Tokyo, 4-6-1 Komaba, Meguro-ku, Tokyo 153-8904, Japan*
[c]*Genome Exploration Research Group, Genome Science Laboratory, Genome Sciences Center, RIKEN, 1-7-22 Suehiro-cho, Tsurumi-ku, Yokohama 230-0045, Japan*

Received 13 December 2002; received in revised form 24 February 2003; accepted 6 March 2003
Received by T. Gojobori

**Abstract**

We have recently reported on two novel human ABC transporters, ABCC11 and ABCC12, the genes of which are tandemly located on human chromosome 16q12.1 [Biochem. Biophys. Res. Commun. 288 (2001) 933]. The present study addresses the cloning and characterization of Abcc12, a mouse orthologue of human ABCC12. The cloned Abcc12 cDNA was 4511 bp long, comprising a 4101 bp open reading frame. The deduced peptide consists of 1367 amino acids and exhibits high sequence identity (84.5%) with human ABCC12. The mouse *Abcc12* gene consists of at least 29 exons and is located on the mouse chromosome 8D3 locus where conserved linkage homologies have hitherto been identified with human chromosome 16q12.1. The mouse *Abcc12* gene was expressed at high levels exclusively in the seminiferous tubules in the testis. In addition to the Abcc12 transcript, two splicing variants encoding short peptides (775 and 687 amino acid residues) were detected. In spite of the genes coding for both ABCC11 and ABCC12 being tandemly located on human chromosome 16q12.1, no putative mouse orthologous gene corresponding to the human *ABCC11* was detected at the mouse chromosome 8D3 locus.


*Keywords:* ATP binding cassette transporter; Mouse; Abcc12; Mouse chromosome 8; Human chromosome 16; Sertoli cell

## 1. Introduction

The ATP-binding cassette (ABC) transporters form one of the largest protein families and play a biologically important role as membrane transporters or ion channel modulators (Higgins, 1992). According to the recently published draft sequence of the human genome, more than 50 human ABC transporter genes (including pseudogenes[1]) are anticipated to exist in the human genome. Hitherto 49 human ABC-transporter genes have been identified and sequenced (recent reviews: Klein et al., 1999; Dean et al., 2001; Borst and Oude Elferink, 2002). Based on the arrangement of their molecular structural components, i.e. the nucleotide binding domain and the topology of transmembrane spanning domains, human ABC transporters are classified into seven different gene families designated as A to G (the new nomenclature of human ABC transporter genes: http://gene.ucl.ac.uk/nomenclature/genefamily/abc.html). Mutations in the human ABC transporter genes have been reported to cause such genetic diseases as Tangier

☆ The cDNA sequences of mouse Abcc12 and its splice variants A and B have been registered in GenBank under the accession numbers of AF502146 (April 12, 2002), AF514414 (May 22, 2002), and AF514415 (May 22, 2002), respectively.

*Abbreviations:* ABC, ATP-binding cassette; EST, expresed sequence tag; MRP, multidrug resistance-associated protein; GAPDH, glutaraldehyde dehydrogenase; GS-X, pump, ATP-dependent glutathione *S*-conjugate export pump; RT–PCR, reverse transcriptase–polymerase chain reaction.

* Corresponding author. Tel.: +81-45-924-5800; fax: +81-45-924-5838.
*E-mail address:* tishikaw@bio.titech.ac.jp (T. Ishikawa).

[1] A truncated human ABC transporter, ABCC13 (GenBank accession number: AF418600), has most recently been cloned (Yabuuchi et al., 2002).

0378-1119/03/$ - see front matter © 2003 Elsevier Science B.V. All rights reserved.
doi:10.1016/S0378-1119(03)00504-3

disease, cystic fibrosis, Dubin–Johnson syndrome, Stargardt disease, and sitosterolemia (recent reviews: Dean et al., 2001; Borst and Oude Elferink, 2002).

We originally reported that transport of glutathione S-conjugates and leukotriene $C_4$ ($LTC_4$) across the cell membrane is mediated by an ATP-dependent transporter named the 'GS-X pump' (Ishikawa, 1989, 1992); however, the molecular nature of the transporter was not uncovered at that time. Later studies have provided evidence that the GS-X pump is encoded, at least, by the ABCC1 (MRP1) gene (Leier et al., 1994; Müller et al., 1994). ABCC1 (MRP1) was first identified by Cole et al. (1992) in the molecular cloning of cDNA from human multidrug-resistant lung cancer cells. After the discovery of the ABCC1 (MRP1) gene, six human homologues, ABCC2 (cMOAT/MRP2), ABCC3 (MRP3), ABCC4 (MRP4), ABCC5 (MRP5), ABCC6 (MRP6), and ABCC10 (MRP7) have been successively identified. Those ABC transporters exhibit a wide spectrum of biological functions and are involved in the transport of drugs as well as endogenous substances (see recent reviews: Borst and Oude Elferink, 2002; Ishikawa, in press).

Most recently, our group (Yabuuchi et al., 2001) and others (Tammur et al., 2001; Bera et al., 2001, 2002) have independently discovered two novel ABC transporters, human ABCC11 (MRP8) and ABCC12 (MRP9), that belong to the ABCC gene family. The predicted amino acid sequences of both gene products show a high similarity with ABCC5. The *ABCC11* and *ABCC12* genes consist of at least 30 and 29 exons, respectively, and they are tandemly located in a tail-to-head orientation on human chromosome 16q12.1 (Yabuuchi et al., 2001; Tammur et al., 2001). The physiological functions of these genes are not yet known; however recent linkage analyses have demonstrated that a putative gene responsible for paroxysmal kinesigenic choreoathetosis (PKC), a genetic disease of infancy, is located in the region of 16p11.2–q12.1 (Lee et al., 1998; Tomita et al., 1999). Since the *ABCC11* and *ABCC12* genes are encoded at that 16q12.1 locus, a potential link between the PKC gene and these ABC transporters has been implicated.

To elucidate the physiological function of human ABCC11 and ABCC12, knockout mice are considered to be a useful animal model. For this reason, we have undertaken the present study to pursue mouse orthologues of ABCC11 and ABCC12. In this study, we have cloned the cDNA of mouse Abcc12 and characterized its chromosomal location, gene organization, tissue-specific expression, the putative protein structure, and splicing variants.

## 2. Materials and methods

### 2.1. Cloning of mouse Abcc 12 cDNA

Mouse EST clones bearing a high similarity to partial sequences of human ABCC 12 cDNA were extracted from the NCBI mouse EST database and the mouse cDNA 'FANTOM 2' database of RIKEN (The FANTOM Consortium, 2002) by using the NCBI BLAST search program (Fig. 1). We have screened multiple tissue cDNA libraries (MTC, Clontech, Palo Alto, CA, USA) by PCR with the following primers deduced from the EST sequences: the forward primer, 5′-AGTTCCCTCATTTCAGCTCTCC-TAGGAC-3′, and the backward primer, 5′-GCAGGTA-GAGCTGACGATTAGCATAC-3′. High expression was detected in mouse testis.

To clone the mouse Abcc12 cDNA from the testis, we have designed four sets of PCR primers, as shown in Fig. 1. The PCR primer sets were as follows: c12-1 (the forward primer: 5′-GCCAAAAGTCGAGGGCTCCAAAACACC-3′ and the backward primer: 5′-GGCCACTGCTTTGACC-GAGAA-3′), c12-2 (the forward primer: 5′-GGCTGGC-TATGTCCAAAGTGGAA-3′ and the backward primer: 5′-GATGCCAAACATCAACACAGACACC-3′), c12-3 (the forward primer: 5′-GATGATGGGCAGCTCTGCTT-TC-3′ and the backward primer: 5′-TCACATGTCCA-TCGCCTCCTCTCA-3′), and c12-4 (the forward primer: 5′- GCCCGACTCTGCATTTGCGA-3′ and the backward primer: 5′-CAAAATCCAGGAACGCTGTCATCTCC-3′). The PCR reaction was performed with mouse testis cDNA (Clontech) and *Ex Taq* polymerase (TaKaRa, Japan), where the reaction consisted of 30 cycles of 95 °C for 30 s, 58 °C for 30 s, and 72 °C for 90 s. After agarose gel electrophoresis, the PCR products were extracted from the gels and subsequently inserted into TA cloning vectors (Invitrogen, Japan). The sequences of the inserts were analyzed with an automated DNA sequencer. (Toyobo Gene Analysis, Japan). The whole cDNA of mouse Abcc12 was obtained by assembling those partial sequences.

### 2.2. Detection of mouse Abcc 12 transcripts by PCR in different tissues

The expression of mouse Abcc 12 in different organs was examined by PCR with the mouse Multiple Tissue cDNA (MTC, Clontech). Two sets of PCR primers were designed to detect the corresponding transcript (Fig. 1), namely, the primer set #1 detecting the 5′-part of Abcc12 cDNA (the forward primer: 5′-CCACTGTCTCCTTATGACTCATCG-GAC-3′, the backward primer: 5′-GGGACAAAACAAGG-CAGCCTCAAAC-3′) and the primer set #2 recognizing the 3′-part of Abcc12 cDNA (the forward primer: 5′-TAT-GGCCCGGGCACTTCTCCGTAA-3′, the backward primer 5′-GACCTTTACAGTCCAACCTCTGCAGCTAGT-3′). The PCR reaction consisted of 35 cycles of 95 °C for 30 s, 58 °C for 30 s, and 72 °C for 30 s. The reaction products were detected by agarose gel electrophoresis.

### 2.3. Northern blot analysis

Mouse organs (i.e. heart, kidney, brain, testis, spleen, stomach, liver, thymus, and small intestine) were surgically

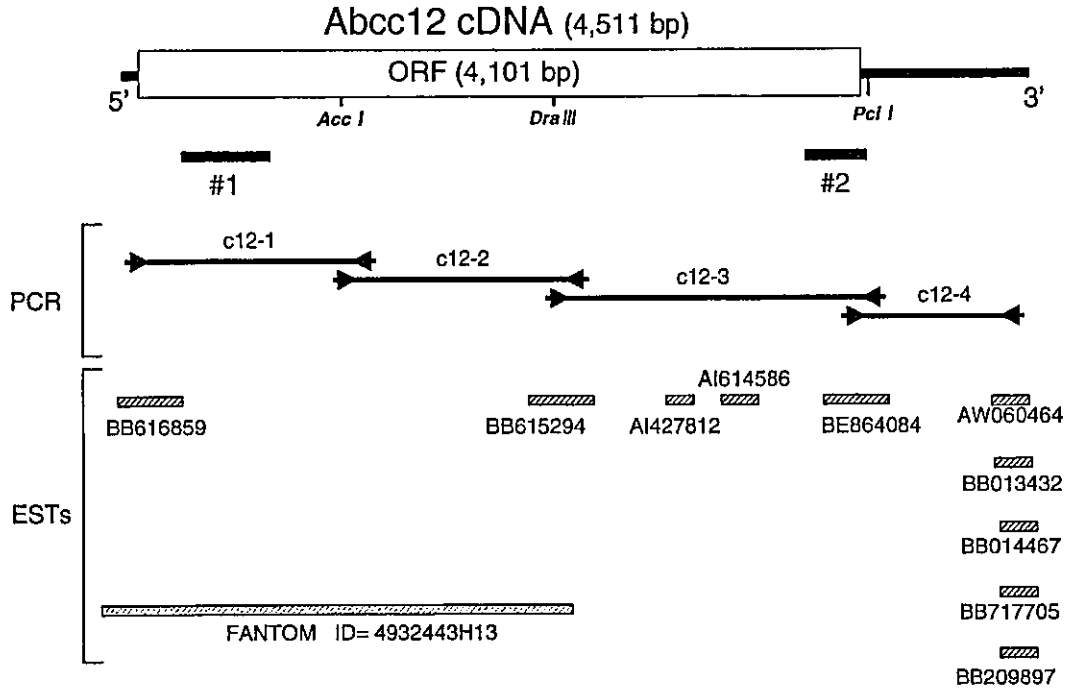


Fig. 1. Strategy for the cloning of mouse Abcc12 cDNA. The open reading frame (ORF) is indicated by a box. The cleavage sites by restriction enzymes (*Acc* I, *Dra* III and *Pci* I) are also indicated. The cDNA was cloned by PCR with four sets of primers, c12-1, c12-2, c12-3, and c12-4, as described in Section 2. The forward and backward PCR primers are indicated by arrows, and the resulting PCR products are represented by straight lines. ESTs and the FANTOM 2 cDNA are sorted according to the sequence homology with Abcc12 cDNA. PCR products used to detect the Abcc12 transcript in different tissues are indicated by #1 and #2.

excised from Balb/C mice (10 weeks old) under anesthesia and immediately frozen in liquid nitrogen. The tissue was pulverized in a mortar containing liquid nitrogen. The resulting tissue powder was subsequently homogenized in TRIzol (Invitrogen, Japan) by using a Polytron homogenizer, and total RNA was extracted according to the manufacturer's protocol. A sample (15 μg/lane as determined by absorbance at 260 nm) of RNA, thus prepared, was subjected to electrophoresis in 1% (w/v) agarose gels containing formaldehyde and then transferred to Hybond-XL membranes (Amersham Pharmacia Biotech). RNA was fixed on the membrane surface by baking at 80 °C for 2 h.

Three different DNA probes encoding partial sequences (463–1165; 1440–2116; 3660–4154) of the Abcc12 cDNA ORF were prepared and separately labeled with [$^{32}$P]dCTP by using the BcaBest labeling kit (TaKaRa) according to the random-primed labeling method. Hybridization with those DNA probes was carried out according to the hybridization protocol of the Expresshybri kit (Clontech), and the hybridization signal was detected in a BASS 2000 (Fuji Film, Japan).

### 2.4. Laser-captured microdissection and RT–PCR

The frozen tissue of mouse testis was cut into thin sections (5 μm thickness) with a microtome (Leika GmbH, Germany) and mounted onto glass slides. The tissue slice on the glass slide was stained in 70% Giemsa solution. After staining, the tissue slices were dehydrated in 100% ethanol and subsequently in 100% xylene. The slide was air-dried, and the seminiferous tubules and the interstitium in the tissue slices were excised by laser-capture microdissection with an Arcturus PixCell 2 LCM system (Arcturus Engineering, Mountain View, CA). The dissected samples were homogenized in 200 μl of TRIzol, and RNA was extracted. mRNA was then converted to cDNA by reverse transcriptase (RT) using a SensiScripts kit (Qiagen). Expression of mouse Abcc12 in these samples was detected by PCR with the same primers and under the same conditions as described in Section 2.2.

### 2.5. In situ hybridization

The testis was surgically excised from mice under anesthesia and immersed in phosphate-buffered saline (PBS) containing 4% paraformaldehyde. The tissue was embedded in paraffin, and thin sections (4 μm thickness) were prepared with a microtome. The resulting thin sections were soaked in xylene three times (3 min for each) and twice in 100% ethanol (3 min for each). Thereafter, sections were rinsed in 70% ethanol and subsequently in 0.1% DEPC-treated water three times. Prior to hybridization, the sections were treated with proteinase K (1:400 v/v) in Tris-buffered saline (TBS) at room temperature for 10 min and

A

```
Mouse Abcc12     1 MVGEGPYLISDLDRRGHRRSFAERYDPSLKTMIPVRPRARLAPNPVDDAGLLSFATFSWL 60
Human ABCC12     1 MVGEGPYLISDLDQRGRRRSFAERYDPSLKTMIPVRPCARLAPNPVDDAGLLSFATFSWL 60

Mouse Abcc12    61 TPVMIRSYKHTLTVDTLPPLSPYDSSDINAKRFQILWEEEIKRVGPEKASLGRVVWKFQR 120
Human ABCC12    61 TPVMVKGYRQRLTVDTLPPLSTYDSSDTNAKRFRVLWDEEVARVGPEKASLSHVVWKFQR 120

Mouse Abcc12   121 TRVLMDVVANILCIVMAALGPTVLIHQILQHITSISSGHIGIGICLCLALFTTEFTKVLF 180
Human ABCC12   121 TRVLMDIVANILCIIMAAIGPTVLIHQILQQTERTSG-KVWVGIGLCIALFATEFTKVFF 179

Mouse Abcc12   181 WALAWAINYRTAIRLKVALSTLIFENLLSFKTLTHISAGEVLNILSSDSYSLFEAALFCP 240
Human ABCC12   180 WALAWAINYRTAIRLKVALSTLVFENLVSFKTLTHISVGEVLNILSSDSYSLFEAALFCP 239

Mouse Abcc12   421 PPSYITQPEDPDTILLLANATLTWEQEINRKSDPPKAQIQKRHVFKKQRPELYSEQSRSD 480
Human ABCC12   420 PPSYITQPEDPDTVLLLANATLTWEHEARQESTPKKLQNQKRHLCKKQRSEAYSERSPPA 479
                                                  Walker A
Mouse Abcc12   481 QGVASPEWQSGSPKSVLHNISFVVRKGKVLGICGNVGSGKSSLISALLGQMQLQKGVVAV 540
Human ABCC12   480 KGATGPEEQSDSLKSVLHSISFVVRKGKILGICGNVGSGKSSLLAALLGQMQLQKGVVAV 539

Mouse Abcc12   541 NGPLAYVSQQAWIFHGNVRENILFGEKYNHQRYQHTVHVCGLQKDLNSLPYGDLTEIGER 600
Human ABCC12   540 NGTLAYVSQQAWIFHGNVRENILFGEKYDHQRYQHTVRVCGLQKDLSNLPYGDLTEIGER 599
                        Signature C      Walker B
Mouse Abcc12   601 GVNLSGGQRQRISLARAVYANRDLYLLDDPLSAVDAHVGKHVFEECIKKTLKGKTVVLVT 660
Human ABCC12   600 GLNLSGGQRQRISLARAVYSDRDLYLLDDPLSAVDAHVGKHVFEECIKKTLRGKTVVLVT 659

Mouse Abcc12   661 HQLQFLESCDEVILLEDGEICEKGTHKELMEERGRYAKLIHNLRGLQFKDPEHIYNVAMV 720
Human ABCC12   660 HQLQFLESCDEVILLEDGEICEKGTHKELMEERGRYAKLIHNLRGLQFKDPEHLYNAAMV 719

Mouse Abcc12   721 ETLKESPAQRDEDAVLASGDEKDEGKEPETEE-FVDTNAPAHQLIQTESPQEGIVTWKTY 779
Human ABCC12   720 EAFKESPAEREEDAVLAPGNEKDEGKESETGSEFVDTKVPEHQLIQTESPQEGTVTWKTY 779

Mouse Abcc12   780 HTYIKASGGYLVSFLVLCLFFLMMGSSAFSTWWLGIWLDRGSQVVCASQNNKTACNVDQT 839
Human ABCC12   780 HTYIKASGGYLLSLFTVFLFLLMIGSAAFSNWWLGLWLDKGSRMTCGPQGNRTMCEVGAV 839

Mouse Abcc12   840 LQDTKHHMYQLVYIASMVSVLMFGIIKGFTFTNTTLMASSSLHNRVFNKIVRSPMSFFDT 899
Human ABCC12   840 LADIGQHVYQRVYTASMVFMLVFGVTKGFVFTKTTLMASSSLHDTVFDKILKSPMSFFDT 899

Mouse Abcc12   900 TPTGRLMNRFSKDMDELDVRLPFHAENFLQQFFMVVFILVIMAAVFPVVLVVLAGLAVIF 959
Human ABCC12   900 TPTGRLMNRFSKDMDELDVRLPFHAENFLQQFFMVVFILVILAAVFPAVLLVVASLAVGF 959

Mouse Abcc12   960 LILLRIFHRGVQELKQVENISRSPWFSHITSSIQGLGVIHAYDKKDDCISKFKTLNDENS 1019
Human ABCC12   960 FILLRIFHRGVQELKKVENVSRSPWFTHITSSMQGLGIIHAYGKKESCIT-Y-------- 1010

Mouse Abcc12  1020 SHLLYFNCALRWFALRMDILMNIVTFVVALLVTLSFSSISASSKGLSLSYIIQLSGLLQV 1079
Human ABCC12  1011 -HLLYFNCALRWFALRMDVLMNILTFTVALLVTLSFSSISTSSKGLSLSYIIQLSGLLQV 1069

Mouse Abcc12  1080 CVRTGTETQAKFTSAELLREYILTCVPEHTHPFKVGTCPKDWPSRGEITFKDYRMRYRDN 1139
Human ABCC12  1070 CVRTGTETQAKFTSVELLREYISTCVPECTHPLKVGTCPKDWPSCGEITFRDYQMRYRDN 1129
                                  Walker A
Mouse Abcc12  1140 TPLVLDGLNLNIQSGQTVGIVGRTGSGKSSLGMALFRLVEPASGTIIIDEVDICTVGLED 1199
Human ABCC12  1130 TPLVLDSLNLNIQSGQTVGIVGRTGSGKSSLGMALFRLVEPASGTIFIDEVDICILSLED 1189

Mouse Abcc12  1200 LRTKLTMIPQDPVLFVGTVRYNLDPLGSHTDEMLWHVLERTFMRDTIMKLPEKLQAEVTE 1259
Human ABCC12  1190 LRTKLTVIPQDPVLFVGTVRYNLDPFESHTDEMLWQVLERTFMRDTTMKLPEKLQAEVTE 1249
                        Signature C      Walker B
Mouse Abcc12  1260 NGENFSVGERQLLCMARALLRNSKIILLDEATASMDSKTDTLVQSTIKEAFKSCTVLTIA 1319
Human ABCC12  1250 NGENFSVGERQLLCVARALLRNSKIILLDEATASMDSKTDTLVQNTIKDAFKGCTVLTIA 1309

Mouse Abcc12  1320 HRLNTVLNCDLVLVMENGKVIEFDKPEVLAEKPDSAFAMLLAAEVGL 1366
Human ABCC12  1310 HRLNTVLNCDHVLVMENGKVIEFDKPEVLAEKPDSAFAMLLAAEVRL 1356
```

Fig. 2. Alignments of the mouse Abcc12 and human ABCC12 proteins. (A) Amino acid sequences were aligned by using the GENETYX-MAC program. The Walker A and B motifs as well as the signature C are indicated by boxes. (B) The hydropathy plots of mouse Abcc12 (this study) and human ABCC12 (Yabuuchi et al., 2001). The hydropathy profiles were calculated according to the Kyte and Doolittle (1982) algorithm.